

RESEARCH ARTICLE

MR-based age-related effects on the striatum, globus pallidus, and thalamus in healthy individuals across the adult lifespan

Stephanie Tullo^{1,2}  | Raihaan Patel^{2,3} | Gabriel A. Devenyi^{2,4}  | Alyssa Salaciak² | Saashi A. Bedford^{1,2} | Sarah Farzin² | Nancy Wlodarski² | Christine L. Tardif⁵  | the PREVENT-AD Research Group⁶ | John C. S. Breitner⁶ | M. Mallar Chakravarty^{1,2,3,4}

¹Integrated Program in Neuroscience, McGill University, Montreal, Quebec, Canada

²Computational Brain Anatomy Laboratory, Cerebral Imaging Centre, Douglas Mental Health University Institute, Verdun, Quebec, Canada

³Department of Biological and Biomedical Engineering, McGill University, Montreal, Quebec, Canada

⁴Department of Psychiatry, McGill University, Montreal, Quebec, Canada

⁵McConnell Brain Imaging Center, Montreal Neurological Institute, McGill University, Montreal, Quebec, Canada

⁶Centre for the Studies on the Prevention of AD, Douglas Mental Health University Institute, Verdun, Quebec, Canada

Correspondence

Stephanie Tullo, Integrated Program in Neuroscience, McGill University, Montreal, Quebec, Canada.
Email: stephanie.tullo@mail.mcgill.ca

M. Mallar Chakravarty, Computational Brain Anatomy Laboratory, Cerebral Imaging Centre, Douglas Mental Health University Institute, Verdun, Quebec, Canada.
Email: mallar@cobralab.ca

Funding information

Fonds de Recherche du Québec - Santé; Natural Sciences and Engineering Research Council of Canada; Weston Brain Institute; Michael J. Fox Foundation; Brain Canada; Alzheimer's Society; Canadian Institutes of Health Research

Abstract

While numerous studies have used magnetic resonance imaging (MRI) to elucidate normative age-related trajectories in subcortical structures across the human lifespan, there exists substantial heterogeneity among different studies. Here, we investigated the normative relationships between age and morphology (i.e., volume and shape), and microstructure (using the T1-weighted/T2-weighted [T1w/T2w] signal ratio as a putative index of myelin and microstructure) of the striatum, globus pallidus, and thalamus across the adult lifespan using a dataset carefully quality controlled, yielding a final sample of 178 for the morphological analyses, and 162 for the T1w/T2w analyses from an initial dataset of 253 healthy subjects, aged 18–83. In accordance with previous cross-sectional studies of adults, we observed age-related volume decrease that followed a quadratic relationship between age and bilateral striatal and thalamic volumes, and a linear relationship in the globus pallidus. Our shape indices consistently demonstrated age-related posterior and medial areal contraction bilaterally across all three structures. Beyond morphology, we observed a quadratic inverted U-shaped relationship between T1w/T2w signal ratio and age, with a peak value occurring in middle age (at around 50 years old). After permutation testing, the Akaike information criterion determined age relationships remained significant for the bilateral globus pallidus and thalamus, for both the volumetric and T1w/T2w analyses. Our findings serve to strengthen and expand upon previous volumetric analyses by providing a normative baseline of morphology and microstructure of these structures to which future studies investigating patients with various disorders can be compared.

KEYWORDS

adult lifespan, basal ganglia, healthy aging, magnetic resonance imaging, microstructure, segmentation, surface-based morphology, thalamus

1 | INTRODUCTION

Certain subcortical structures of the brain, such as the striatum and thalamus, are implicated in many aspects of motor function and cognition (Middleton & Strick, 2000), and are critically involved in several domains of everyday functioning (Graybiel, 1995). The basal ganglia, which include the striatum and globus pallidus, are positioned deep below the cortical manifold and serve as important network hubs and relays, precisely modulating the neuronal activity of several functional systems involved in psychomotor behavior (Parent & Hazrati, 1995). These structures contain numerous laminae and myelinated fibers differentially synapsing within subnuclei, and have multiple reciprocal connections between one another, as well as to regions implicated in complex cognitive tasks such as the frontal cortex (Jahanshahi, Obeso, Rothwell, & Obeso, 2015; Leh, Ptito, Chakravarty, & Strafella, 2007). Moreover, abnormalities in these subcortical structures have been implicated in neuropsychiatric disorders (e.g., schizophrenia, depression; Abi-Dargham & Meyer, 2014; Chakravarty et al., 2015; Hannestad et al., 2006; Howes & Kapur, 2009; Makowski et al., 2018; Nauczyciel et al., 2013), movement disorders (e.g., Parkinson's disease, Huntington's disease; Alexander, DeLong, & Strick, 1986; Aylward et al., 1997; Graybiel, 2000; Obeso et al., 2000), and addictions and habit forming behaviors (Belin, Jonkman, Dickinson, Robbins, & Everitt, 2009; Garza-Villarreal et al., 2017; Yin & Knowlton, 2006).

While numerous studies have used magnetic resonance imaging (MRI) to demonstrate subcortical volumetric age relationships occurring across the lifespan in vivo (Courchesne et al., 2000; Brain Development Cooperative Group, 2012; Fjell et al., 2013; Fotenos, Snyder, Girton, Morris, & Buckner, 2005; Good et al., 2001; Goodro, Sameti, Patenaude, & Fein, 2012; Greenberg et al., 2008; Guadalupe et al., 2017; Inano et al., 2013; Jäncke, Méritat, Liem, & Hänggi, 2015; Jernigan et al., 2001; Narvacan, Treit, Camicioli, Martin, & Beaulieu, 2017; Potvin et al., 2016; Raz et al., 2003, 2005; Raz & Rodrigue, 2006; Raznahan et al., 2014; Sullivan, Rosenbloom, Serventi, & Pfefferbaum, 2004; Tamnes et al., 2013; Van Der Werf et al., 2001; Walhovd et al., 2005, 2011; Ziegler et al., 2012), there are several discrepancies between the trajectories that have been previously reported. Different age-related relationships have been observed, with some studies suggesting linear decline beginning early in life (Fjell et al., 2013; Goodro et al., 2012; Greenberg et al., 2008; Gunning-Dixon, Head, McQuain, Acker, & Raz, 1998; Inano et al., 2013; Raz et al., 2003; Sullivan et al., 2004; Van Der Werf et al., 2001; Walhovd et al., 2005, 2011), whereas others report quadratic trajectories, with an increase in volume followed by a subsequent decline (Fjell et al., 2013; Goodro et al., 2012; Inano et al., 2013; Narvacan et al., 2017; Potvin et al., 2016; Walhovd et al., 2005, 2011), or cubic relationships, with differing results denoting the peak of volume attainment (Fjell et al., 2013; Potvin et al., 2016).

Diverging results across studies may likely be the result of the diverse methods used for the accurate visualization and delineations of the subcortical structures using MRI. Specifically, these studies use various segmentation techniques (manual or computer-assisted methods (Greenberg et al., 2008; Gunning-Dixon et al., 1998; Jernigan et al.,

2001; Raz et al., 2003, 2005; Sullivan et al., 2004; Van Der Werf et al., 2001), FreeSurfer (Fischl et al., 2002; <http://surfer.nmr.mgh.harvard.edu>) (Fjell et al., 2013; Guadalupe et al., 2017; Inano et al., 2013; Jäncke et al., 2015; Narvacan et al., 2017; Potvin et al., 2016; Tamnes et al., 2013; Walhovd et al., 2005, 2011), FSL-FIRST (Patenaude, Smith, Kennedy, & Jenkinson, 2011; <http://fsl.fmrib.ox.ac.uk>) (Goodro et al., 2012)), all of which have differing segmentation criteria and definitions of the underlying anatomy. Most early studies examining the effects of normal aging on subcortical structures have utilized manual segmentation to delineate their structures of interest, whereas most recent studies have utilized automated segmentation methods. Furthermore, the data were acquired using different scanning acquisitions parameters (field strength differences [1.5 T vs. 3 T], voxel dimensions, etc...). Both of these methodological parameters have been shown to influence tissue-specific signal (leading to differential contrast between at structure boundaries) and border visibility (Fushimi et al., 2007; Pfefferbaum, Rohlfing, Rosenbloom, & Sullivan, 2012), and therefore may have potential confounding effects on measures of volume. This inconsistency is particularly prevalent for the studies involving the basal ganglia. The basal ganglia tend to accumulate more inorganic inclusions (e.g., calcification or iron deposits), in comparison to other subcortical structures commonly investigated (Raz et al., 2003), and these deposits have effects on the MR signal (due to the ferromagnetic property of the iron) that differ depending on the field strength of the MRI machine (Pfefferbaum et al., 2012).

Previous MR-based investigations of the relationship between subcortical anatomy and age have typically focused on volumetry; however, there are exceptions (Callaghan et al., 2014 [voxel-based quantification]; Cherubini, Pérán, Caltagirone, Sabatini, & Spalletta, 2009 [volume, iron deposition, and microstructural damage]; Raznahan et al., 2014 [shape analyses]; Xu, Wang, & Zhang, 2008 [iron deposition]; Ziegler et al., 2012 [voxel-based morphometry]). Notably, mapping subcortical shape, specifically surface area can be used to pinpoint neuroanatomical alterations that may be complementary to or even more sensitive than traditional volumetric measures. A recent study by Raznahan et al. (2014) examined subcortical shape, in addition to volume, in typically developing males and females between the ages of 5 and 25 years, using the MAGeT-Brain subcortical morphology pipeline (Chakravarty et al., 2013; Pipitone et al., 2014). They observed that striatal, pallidal, and thalamic subdomains typically described as being connected to frontoparietal association cortices contract with age, and demonstrated a nuanced and multidimensional description of age-related subcortical morphological relationships.

Given that T1w and T2w images are commonly acquired in many neuroimaging studies, and the T1w/T2w signal ratio technique can be used as an estimate of the underlying microstructure, where the signal contribution comes, in part, from myelin. This putative and controversial (see section 4) MR-accessible proxy of myelin is based on the principle that the signal intensity of T1w and T2w images are assumed to be directly and inversely proportional to myelin contrast, respectively.

The objective of this study is to investigate the normative relationships between age and subcortical volume across the adult lifespan in healthy individuals between the ages of 18 and 83 using structural

MRI. In addition, a unique contribution of this manuscript is the complementary analyses of microstructure and surface-based morphometry measures of the striatum, globus pallidus, and thalamus in order to achieve a multi-dimensional normative baseline across several indices related to microstructure and morphology. Furthermore, we sought to examine a potential factor related to the different age trajectories reported in the literature; the effect of quality control (QC) and segmentation accuracy. Recent work from our group, Bedford et al. (2019), and others (Ducharme et al., 2016) demonstrate that varying levels of QC alter cortical thickness age trajectories radically. When implementing strict QC criteria, both studies report previously observed higher order trajectories were mostly replaced by linear effects. Given that details about data exclusion from QC procedures are underreported, lenient or nonexistent QC procedures may account for spurious findings, contributing to the lack of reproducibility of the findings in subsequent investigations, and possibly playing a significant role in the inconsistency of volumetry results reported in the healthy aging literature.

2 | METHODS

2.1 | Subjects demographics

A total of 253 healthy individuals (107 males and 146 females, mean age = 58.2 ± 15.6 , age range: 18–83) were recruited across two studies: as part of a study investigating the effects of normal and healthy aging on neuroanatomy (Healthy Aging [HA] Study), or as a control group in a study investigating high-resolution MRI-based biomarkers for identifying risk for Alzheimer's disease (Alzheimer's Disease Biomarkers [ADB] Study). Table 1 describes summary subject characteristics for the two studies (prequality and postquality control). All

participants provided signed informed consent to participate in either study, both of which were approved by the Research Ethics Board of the Douglas Mental Health University Institute, Montreal, QC, Canada. Individuals with a history of neurological or psychiatric illness, physical injuries such as head trauma and concussion, alcohol/substance abuse or dependence, and current drug use were excluded. The cognitive status of the participants was evaluated using the MMSE (Mini Mental State Examination) for the HA Study, and the MMSE and MoCA (Montreal Cognitive Assessment) for the healthy controls in the ADB Study. Subjects with a MMSE score $\geq 24/30$ and a MoCA $\geq 26/30$ were considered eligible. All participants were also evaluated using the Repeatable Battery for the Assessment of Neuropsychological Status (RBANS, Version A; Randolph, Tierney, Mohr, & Chase, 1998). This 30-min battery yields Index Scores in five cognitive domains: Language, immediate memory, delayed memory, attention, and visuospatial abilities, as well as a Total Score. The Wechsler Abbreviated Scale of Intelligence (WASI; Weschler, 1999) was used to obtain a general indication of cognitive functioning for all participants in the Healthy Aging Study. Participant performance on two tasks of the WASI, the vocabulary task and the matrix reasoning task, were converted to age group-specific T-scores and summed to yield a full-scale intelligence quotient (IQ) score. Cognitive ability of the participants from the two studies is characterized in Table 1.

2.2 | Imaging data acquisition

All participants were imaged on a Siemens Trio 3 T MRI scanner using a 32-channel head coil. T1w structural images were acquired using the Alzheimer's Disease Neuroimaging Initiative (ADNI) magnetization-prepared rapid acquisition gradient echo (MPRAGE)

TABLE 1 Subject demographics

	Pre-QC			Post-QC for morphological analyses			Post-QC for T1w/T2w analyses		
	Total	HA	ADB	Total	HA	ADB	Total	HA	ADB
N	253	106	147	178	90	88	162	87	75
Mean age (years) (\pm SD)	58.2 (15.6)	46.2 (16.5)	66.9 (6.3)	54.9 (15.7)	44.5 (15.4)	65.6 (5.8)	54.3 (16.2)	44.2 (15.4)	66.1 (5.9)
Sex (female:male)	146:107	57:49	89:58	110:68	52:38	58:30	101:61	51:36	50:25
Handedness (# right-handers)	188	106	82	141	90	51	137	87	50
Average number of years of education (\pm SD)	16.4 (3.4)	16.6 (3.3)	16.3 (3.4)	16.7 (3.4)	16.6 (3.4)	16.7 (3.4)	16.6 (3.4)	16.7 (3.4)	16.6 (3.5)
MMSE (\pm SD)	28.6 (1.5)	28.8 (1.3)	28.4 (1.6)	28.8 (1.4)	29.0 (1.2)	28.6 (1.6)	28.8 (1.4)	29.0 (1.2)	28.5 (1.6)
MOCA (\pm SD)	NA	NA	26.4 (2.7)	NA	NA	26.5 (2.6)	NA	NA	26.3 (2.7)
RBANS (\pm SD)	99.9 (13.2)	101.6 (14.1)	98.7 (12.4)	101.2 (13.5)	102.8 (13.7)	99.7 (13.3)	101.4 (13.6)	103.2 (13.5)	99.4 (13.6)
WASI (IQ) (\pm SD)	NA	104.3 (18.9)	NA	NA	103.9 (18.1)	NA	NA	104.6 (17.8)	NA

Note. Summary subject characteristics for the total sample, as well as the two studies (Healthy Aging Study [HA] and Alzheimer's Disease Biomarker Study [ADB]) separately, for all subjects prior to any quality control (QC; pre-QC) and for all subjects that passed quality controls for each of the two analyses conducted (Post-QC for Morphological Analyses & Post-QC for T1w/T2w Analyses). For the morphological analyses (i.e., volume and shape analyses), subjects were excluded first based on the motion/artifacts QC scores in the T1w images, and then based on score of accuracy of MAGeT label outputs. For the T1w/T2w analyses, subjects were excluded based on the motion/artifacts QC scores in T1w and T2w images, and based on score of accuracy of MAGeT label outputs.

Abbreviations: IQ, intelligence quotient; MMSE, Mini Mental State Examination; MoCA, Montreal Cognitive Assessment; RBANS, Repeatable Battery for the Assessment of Neuropsychological Status; SD, standard deviation; WASI, Wechsler Abbreviated Scale of Intelligence.

protocol (TE/TR = 2.98 ms/2,300 ms, TI = 900 ms, $\alpha = 9^\circ$, $256 \times 240 \times 176$ matrix, GRAPPA of 2, bandwidth = 238 Hz/pixel, 1.00 mm isotropic voxel dimensions, and scan time 5:12; Jack Jr et al., 2008) for all 253 participants. Two T2w MR images were acquired using a turbo spin echo sequence (TE/TR = 198 ms/2500 ms, $350 \times 263 \times 350$ mm³, phase partial Fourier 6/8, GRAPPA of 2, turbo factor = 87, bandwidth = 781 Hz/pixel, 0.64 mm isotropic voxel dimensions, and scan time 13:22) for the individuals that participated in the HA study ($N = 106$; mean age = 46.2 ± 16.5 , 49 males and 57 females), whereas one T2w image was acquired using the same acquisition, with a single average and partial Fourier to shorten acquisition time (scan time 10:02) for the individuals that participated in the ADB study ($N = 145$; mean age = 66.9 ± 6.3 , 58 males and 87 females). Specifically, the slice partial Fourier was set to 6/8 in the ADB study in order to shorten the acquisition time to about 10 min given that this acquisition sequence is particularly sensitive to motion, and decreasing acquisition time would aid in reducing subject motion. While this change comes at a slight cost in image quality, mainly signal-to-noise ratio, there should be no effect on image contrast (Feinberg, Hale, Watts, Kaufman, & Mark, 1986).

2.3 | Image processing

2.3.1 | Preprocessing

To obtain volume and surface-based metrics, T1w images were preprocessed using the `minc-bpipe-library` (<https://github.com/CobraLab/minc-bpipe-library>) for improved segmentation accuracy. This preprocessing pipeline consisted of a N4 nonuniformity correction (Tustison et al., 2010) and brain extraction, which was performed using the BEaST algorithm (Eskildsen et al., 2012) and used to obtain a measure of total brain volume.

For subjects where two T2w images were acquired, the two T2w images were rigidly aligned, using `antsRegistration` from the Advanced Normalization Tools (ANTs) registration and segmentation toolkit (<http://stnava.github.io/ANTs/>), and then averaged for improved signal-to-noise. No additional preprocessing was performed on the T2w images since native T1w and T2w images are required for the creation of the T1w/T2w images (Glasser & Van Essen, 2011).

2.3.2 | Quality control

All images were visually inspected by one rater (ST) for artifacts. Images with motion artifacts were discarded following the QC procedure implemented by our group, as described in Bedford et al. (2019), and can be found on our GitHub page, <https://github.com/CobraLab/documentation/wiki/Motion-Quality-Control-Manual>. All segmentations were quality controlled by visual inspection, such that all labels that were not deemed accurate were excluded from the statistical analyses, following the QC procedure implemented by our group ([https://github.com/CobraLab/documentation/wiki/MAGeT-Brain-Quality-Control-\(QC\)-Guide](https://github.com/CobraLab/documentation/wiki/MAGeT-Brain-Quality-Control-(QC)-Guide)). Table S1 describes the exclusion rate at each QC step.

After QC, we obtain a final sample of 178 subjects for the volume and shape analyses, and a final sample of 162 subjects for the T1w/T2w analyses. These final samples were used for all subsequent analyses, except for those detailed in Section 3.6. "Impact of QC on Age Trajectories". See Table 1 for a summary of subject characteristics post-QC for both the morphological (volume and shape) and T1w/T2w analysis. See Figure S1 for age histograms pre- and post-QC.

2.3.3 | Volume and shape measures

The preprocessed T1w images were segmented using `MAGeT-Brain`, a multi-atlas registration-based segmentation tool (Chakravarty et al., 2013; Pipitone et al., 2014). Five high-resolution T1w MRI atlases of the striatum, globus pallidus, and thalamus were used (Chakravarty, Bertrand, Hodge, Sadikot, & Collins, 2006; Tullo et al., 2018) to derive subject-based segmentations for all subjects. Structure volumes were extracted from the resulting label images. Surface-based metrics, specifically surface area, were generated by the `MAGeT-Brain` pipeline for the left and right striatum, globus pallidus, and thalamus using a surface mapping technique previously described (Makowski et al., 2018; Raznahan et al., 2014; Shaw et al., 2014, 2015).

To reduce the number of participants excluded due to segmentation inaccuracies, we sought to improve the registrations generated by our automated segmentation pipeline, `MAGeT-Brain`, in an effort to improve the accuracy of the subject-based segmentation generated. Specifically, two implementations were added to improve the registration between the atlases and the subject images; the first was separating the left and right hemisphere, and the second was masking the registration to focus on the areas of interest (Chakravarty et al., 2009; Chakravarty, Sadikot, Germann, Bertrand, & Collins, 2008). These implementations improve the registration by limiting the constraints on the source to target matching of the entire image. See Figure S2 for an example of the output from the `MAGeT-Brain` segmentation pipeline, and the improved segmentation output using the newest implementation of `MAGeT-Brain` with the improved registration technique.

2.3.4 | T1w/T2w measures

In addition to subcortical morphology (i.e., volume, surface area), we evaluated the T1w/T2w signal intensity ratio (Glasser & Van Essen, 2011) to examine microstructure. The ratio of the T1w and T2w images of a subject provides a unitless quantity that has been shown to correlate with myelination (Glasser, Goyal, Preuss, Raichle, & Van Essen, 2014; Glasser & Van Essen, 2011; Grydeland, Walhovd, Tamnes, Westlye, & Fjell, 2013; Shafee, Buckner, & Fischl, 2015; Uddin et al., 2018; Uddin, Figley, Solar, Shatil, & Figley, 2019), however, iron and inflammation have also been observed to contribute to MR image contrast (Tardif et al., 2016). Therefore, in the context of this manuscript, we use T1w/T2w signal ratio as a general microstructure index that is at least partially correlated with myelin.

To enable voxel-by-voxel correspondence between the native T1w and T2w images for the creation of the T1w/T2w images, native T2w

images (either the averaged or single image) were rigidly matched to the native T1w image for each subject (Collins, Neelin, Peters, & Evans, 1994). However, since the voxel dimensions in the T1w and T2w images are different ($1 \times 1 \times 1 \text{ mm}^3$ and $0.64 \times 0.64 \times 0.64 \text{ mm}^3$, respectively), before performing the rigid registration, the T1w images were upsampled to 0.64 mm isotropic voxel dimensions with a windowed sinc interpolation. T1w/T2w outliers were detected and corrected using a variant of the method implemented by Glasser and Van Essen (2011), as this method was developed for filtering cortical surface based T1w/T2w values. Voxels within the three regions of interest that had a T1w/T2w value over two standard deviations from the mean of their neighborhood (which includes 12 voxels in each of x , y , z directions) were detected and corrected by replacing the value with a Gaussian-weighted average of the neighboring voxels, using a three-dimensional Gaussian weighting (FWHM = 5 mm). The mean of the T1w/T2w voxel intensities within each structure label was then computed for each subject.

2.4 | Statistical analyses

Statistical analyses investigating how age predicts subcortical volumes was performed using general linear models (GLM) in R (<https://www.r-project.org>), with total brain volume and sex as covariates. The model was applied individually to each structure, and was performed separately for the left and right hemisphere.

A vertex-wise linear regression was performed to examine local surface area across the adult lifespan, using the same model as the volume analyses. False discovery rate (FDR; Benjamini & Hochberg, 1995) was performed on the vertex-wise analyses of surface area to correct for multiple comparisons. Results are displayed between the 1 and 5% FDR threshold.

A mixed effects model was performed to examine the relationship between age and T1w/T2w for each structure of interest, separately for each hemisphere. We modeled T2w acquisition type as a two level random factor to control for possible differences in signal intensity due to the slightly different T2w acquisition parameters, while taking advantage of expected comparability of age-related effects (Fennema-Notestine et al., 2007).

Volumetric and T1w/T2w analyses were first tested for the best fit using linear, quadratic, and cubic age terms using the Akaike information criterion (AIC; Akaike, 1974). AIC was used to compare models and select the most probable age relationships from multiple fits (linear, quadratic, and cubic) for each structure of interest. The fit with the lowest AIC was chosen as the best fit model, which was performed and reported for each structure Wagenmakers & Farrell, 2004.

Permutation testing was performed by permuting each variable of interest in the linear model for each structure, for both the volumetric and microstructural analyses. A total of 10,000 permutations were used to yield an accurate assessment of the probability of false positive when examining the AIC-determined relationship with age, under the null hypothesis that the labels are interchangeable (Bernal-Rusiel et al., 2013; Knijnenburg, Wessels, Reinders, & Shmulevich, 2009). Using this estimated distribution, p values were calculated for each

subcortical structure, obtained using the `lmp` and `lmm.perm` functions in R for general linear models and mixed effects models respectively. The p -value is the probability of obtaining a result similar to the test statistic given that the null hypothesis is true, such that low p values indicate that the labels are not interchangeable and that the original label configuration is relevant with respect to the data (Knijnenburg et al., 2009). The p -value is assessed by performing all possible permutations and computing the fraction of permutation values that are at least as extreme as the test statistic obtained from the unpermuted data (Knijnenburg et al., 2009).

2.4.1 | Examining the effect of education on age relationships

Since the relationship between education and brain morphology is well-known in the aging and neurodegeneration literature (Fotenos, Mintun, Snyder, Morris, & Buckner, 2008; Mungas et al., 2018; Querbes et al., 2009; Solé-Padullés et al., 2009), the analyses were repeated with years of education as an added covariate (see Section 3.4 and Supplementary Results Section for more details).

2.4.2 | Examining the effect of sex

Each of the models performed and reported in the manuscript were chosen using AIC, such that the best fit model for these data, occurred when modeling sex as covariate, in comparison to when modeling an age by sex interaction (regardless of the fit age term [linear, quadratic, cubic]). However, given that some studies report sex effects in the aging literature (Coffey et al., 1998; Good et al., 2001; Guadalupe et al., 2017; Murphy et al., 1996; Pfefferbaum et al., 2013; Van der Werf et al., 2001; Xu et al., 2000; and other do not; Abedelahi, Hasanzadeh, Hadizadeh, & Joghataie, 2013; Fjell et al., 2009; Giedd et al., 1996; Greenberg et al., 2008; Lemaître et al., 2005; Narvacan et al., 2017; Raz et al., 2003; Sullivan et al., 2004; Wyciszkiwicz & Pawlak, 2014), we nonetheless examined whether there was a significant age by sex interaction in each of the models for each analysis (volume, surface area, and T1w/T2w), where once again AIC was used to determine the best fit for the age term (see Section 3.5 and Supplementary Results Section for more details).

2.4.3 | Examining the impact of QC on volumetric age relationships

Given the diverging results of age–volume relationships reported in the healthy aging literature, we sought to examine a potential factor contributing to the inconsistent volumetry results observed: Varying levels of segmentation accuracy. Across the literature, various segmentation pipelines were used (manual segmentation, FreeSurfer, FSL, etc ...), and there is little to no mention of the QC procedures that were used to assess segmentation accuracy and quality in addition to a description of the subjects that failed QC from the analyses. Increasingly, we see a growing need to address this confound as a means of increasing transparency and improving reproducibility (Backhausen

et al., 2016; Ducharme et al., 2016; Keshavan et al., 2018; Makowski et al., 2018; Shehzad et al., 2015).

To assess the potential impact of exclusion based on segmentation accuracy, we compared the results obtained for the volume analyses on the subset of the subjects that participated in the ADB study (a representative sample of subjects that passed T1w motion QC [$n = 65$ subjects]) when using three different methods of segmentation; (a) manual correction of the automated segmentation generated using MAGeT-Brain ($n = 65$); (b) using the original version of MAGeT ($n = 47$); (c) using the improved version of MAGeT (i.e., with the changes made to improve atlas-to-subject registration, as described in the methods section; $n = 53$). Table 2 describes summary subject characteristics for each of the three QC samples.

Statistical analyses investigating the age–volume relationship was performed as previously described above, using GLMs with total brain volume and sex as covariates, and AIC was used to determine the best fit using linear, quadratic, and cubic age terms using AIC.

3 | RESULTS

3.1 | Relationship between subcortical volume and age

All three subcortical structures showed significant volume–age relationships bilaterally. Figure 1 shows the scatter plots for the relationship between age and volume for the left and right striatum, globus pallidus, and thalamus across the entire adult lifespan. After assessing linear, quadratic, and cubic age terms with the AIC, the linear model was the best fit for the globus pallidus (left: $F(df) = 27.9 (3,173)$; $p = 8.98E-11$; $R^2 = .315$; right: $F(df) = 19.2 (3,173)$; $p < 2.2E-16$; $R^2 = .237$), whereas the quadratic model was the best fit for the striatum and thalamus (all associations held bilaterally; left striatum: $F(df) = 64.0 (4,172)$; $p < 2.2E-16$; $R^2 = .589$; right striatum: $F(df) = 59.1 (4,172)$; $p < 2.2E-16$; $R^2 = .569$; left thalamus: $F(df) = 82.5 (4,172)$; $p < 2.2E-16$; $R^2 = .649$; right thalamus: $F(df) = 80.6 (4,172)$; $p < 2.2E-16$; $R^2 = .644$). These findings are consistent with findings from previous brain imaging studies

(Goodro et al., 2012; Greenberg et al., 2008; Gunning-Dixon et al., 1998; Hasan, Halphen, Boska, & Narayana, 2008; Inano et al., 2013; Jernigan et al., 2001; Raz et al., 2005; Sullivan et al., 2004; Walhovd et al., 2005).

GLM analyses showed significant linear age effects for the globus pallidus (left: $t = -3.34$, $p = .00102$; right: $t = -2.20$, $p = .0295$) and significant quadratic age effects for the thalamus (left: $t = -2.46$, $p = .0148$; right: $t = -2.58$, $p = .0108$) volumes; however, no significant quadratic age effects were observed for the striatum. Exploratory analyses of the linear age term in the best fit quadratic model for the striatum revealed significant linear age effects (left: $t = -7.14$, $p = 2.56E-11$; right: $t = -6.62$, $p = 4.44E-10$). See Figure S3 for linear volume–age relationship for the bilateral striatum. After permutation testing, the AIC-determined models remained significant for all three structures of interest bilaterally (left striatum: $p = <2E-16$; right striatum: $p = <2E-16$; left globus pallidus: $p = <2E-16$; right globus pallidus: $p = .0474$; left thalamus: $p = .0168$; right thalamus: $p = .0106$).

3.2 | Relationship between subcortical shape and age

When examining the relationship between age and surface area across the adult lifespan, we observed linear age-related regional surface areal expansion and contraction in all three structures of interest bilaterally. These results were relatively symmetrical between the hemispheres for all three structures of interest; however, this was observed to a lesser extent for the globus pallidus.

For the striatum, we observed a ventral/dorsal dichotomy, wherein we observed age-related linear surface area contraction on the dorsal side with areal expansion on the ventral side. Specifically, at the 1% FDR level, striatal area contraction with age is most evident in the anterior part of the striatum, in the anterior caudate nucleus and nucleus accumbens regions, as well as in the medial posterior regions of the putamen (left striatum: $t = 2.91$; right striatum: $t = 2.87$). Additionally, striatal areal expansion was observed along the medial surface of the entire anterior–posterior axis of the caudate nucleus, with strong age effects on the dorsal region of the tail of the caudate nucleus.

TABLE 2 Subject demographics of QC analyses

	All subjects that passed motion QC (using manually corrected labels) ($n = 65$)	Subjects that passed motion QC and original MAGeT QC ($n = 47$)	Subjects that passed motion QC and improved MAGeT QC ($n = 53$)	Total ADB (post-QC for morphological analyses)
N	65	47	53	88
Mean age (years) (\pm SD)	68.0 (6.5)	66.3 (5.9)	37.1 (5.9)	65.6 (5.8)
Sex (female:male)	37:28	30:17	31:22	58:30
Handedness (# right-handers)	57	41	41	51
Average number of years of education (\pm SD)	16.4 (4.0)	16.6 (4.0)	16.7 (3.9)	16.7 (3.4)
MMSE (\pm SD)	28.3 (1.8)	28.7 (1.6)	28.5 (1.5)	28.6 (1.6)
MOCA (\pm SD)	35.4 (2.9)	25.6 (2.8)	25.3 (2.8)	26.5 (2.6)
RBANS (\pm SD)	97.1 (14.4)	97.9 (13.0)	97.1 (15.0)	99.7 (13.3)

Abbreviations: IQ, intelligence quotient; MMSE, Mini Mental State Examination; MoCA, Montreal Cognitive Assessment; RBANS, Repeatable Battery for the Assessment of Neuropsychological Status; SD, standard deviation; WASI, Wechsler Abbreviated Scale of Intelligence.

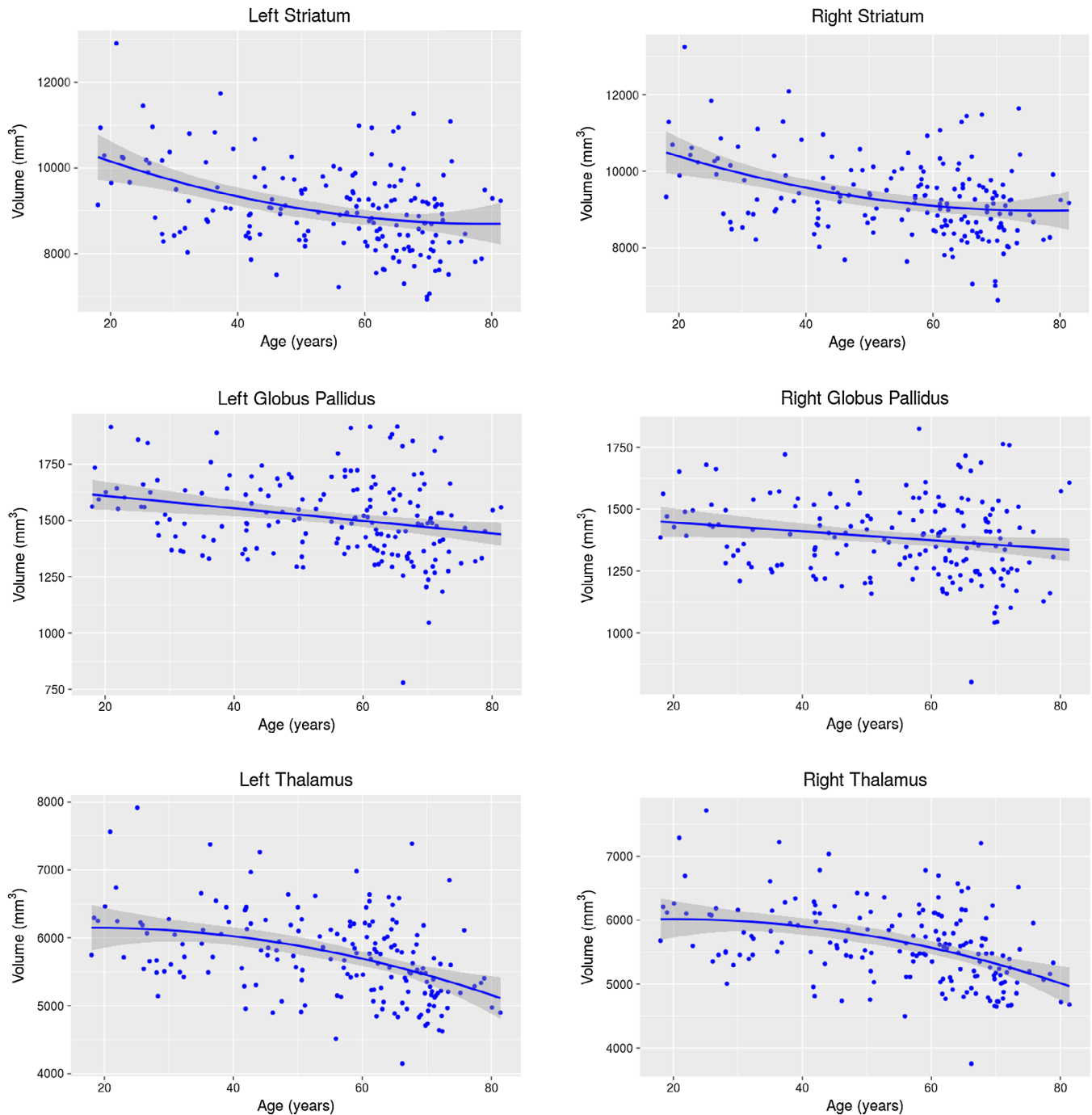


FIGURE 1 Age-related changes in volume. Regression plots showing the relationships between age and the volume for the striatum, globus pallidus, and thalamus. Negative linear relationships were revealed to be the best fit model, as determined by AIC, for the globus pallidus (left: $p = .00102$; right: $p = .0295$), whereas a quadratic relationship was the best fit model for the thalamus (left: $p = 0.0148$; right: $p = 0.0108$). No significant quadratic age effects were observed for the striatum, despite being the best fit model as determined by AIC; see Figure S3 for linear age effects for the bilateral striatum volume [Color figure can be viewed at wileyonlinelibrary.com]

The pallidum also shows an areal contraction with age in the posterior regions, predominantly localized to the medial regions of the left and right globus pallidus. However, for the right globus pallidus, we also observed a pronounced age-related areal contraction on the dorsal region of this structure. The effect of age on pallida surface area was observed at the 1% FDR level (left: $t = 2.83$; right: $t = 2.87$).

Finally, at the 1% FDR level, the thalamus shows a widespread pattern of age-related areal contraction in the posterior regions bilaterally, specifically at the posterior end and in the ventral posterior region, as well as bilaterally in the anterior medial regions of the nucleus (left: $t = 2.77$; right: $t = 2.73$). See Figure 2 for regions where a significant surface area–age relationship was observed.

3.3 | Relationship between subcortical T1w/T2w signal ratio and age

AIC was performed to determine the best fit age model curves between linear, quadratic, or cubic. The quadratic model was the best fit for all structures bilaterally. We observed an initial increase followed by a subsequent decline of average T1w/T2w, with a peak average T1w/T2w occurring at mid-life for all three structures bilaterally. The peak average T1w/T2w occurs at around 50 years old for the left and right striatum, whereas the peak occurs earlier, at around 45 years old, in the left and right globus pallidus and thalamus.

Quadratic age-related relationships with average T1w/T2w were observed bilaterally in the striatum (left: $t = -4.35$, $p = 2.43E-5$; right: $t = -4.94$, $p = 1.95E-6$), globus pallidus (left: $t = -2.65$, $p = .00891$;

right: $t = -3.327$, $p = .00109$), and thalamus (left: $t = -3.66$, $p = .000341$; right: $t = -3.95$, $p = .000116$). Figure 3 shows the scatter plots for the relationship between age and average T1w/T2w for all three subcortical structures bilaterally. Figure S4 shows the contribution of the T1w and T2w signal intensity to the T1w/T2w ratio for each subject across the adult age span.

After permutation testing, the AIC-determined quadratic age relationships remained significant for the globus pallidus and thalamus bilaterally (left globus pallidus: $p = .0133$; right globus pallidus: $p = .0201$; left thalamus: $p = .0026$; right thalamus: $p = .0058$); however, for the striatum, while the left striatum demonstrates a trend toward significance (left striatum: $p = .0702$), the right striatum is no longer significant after permuting the model (right striatum: $p = .166$).

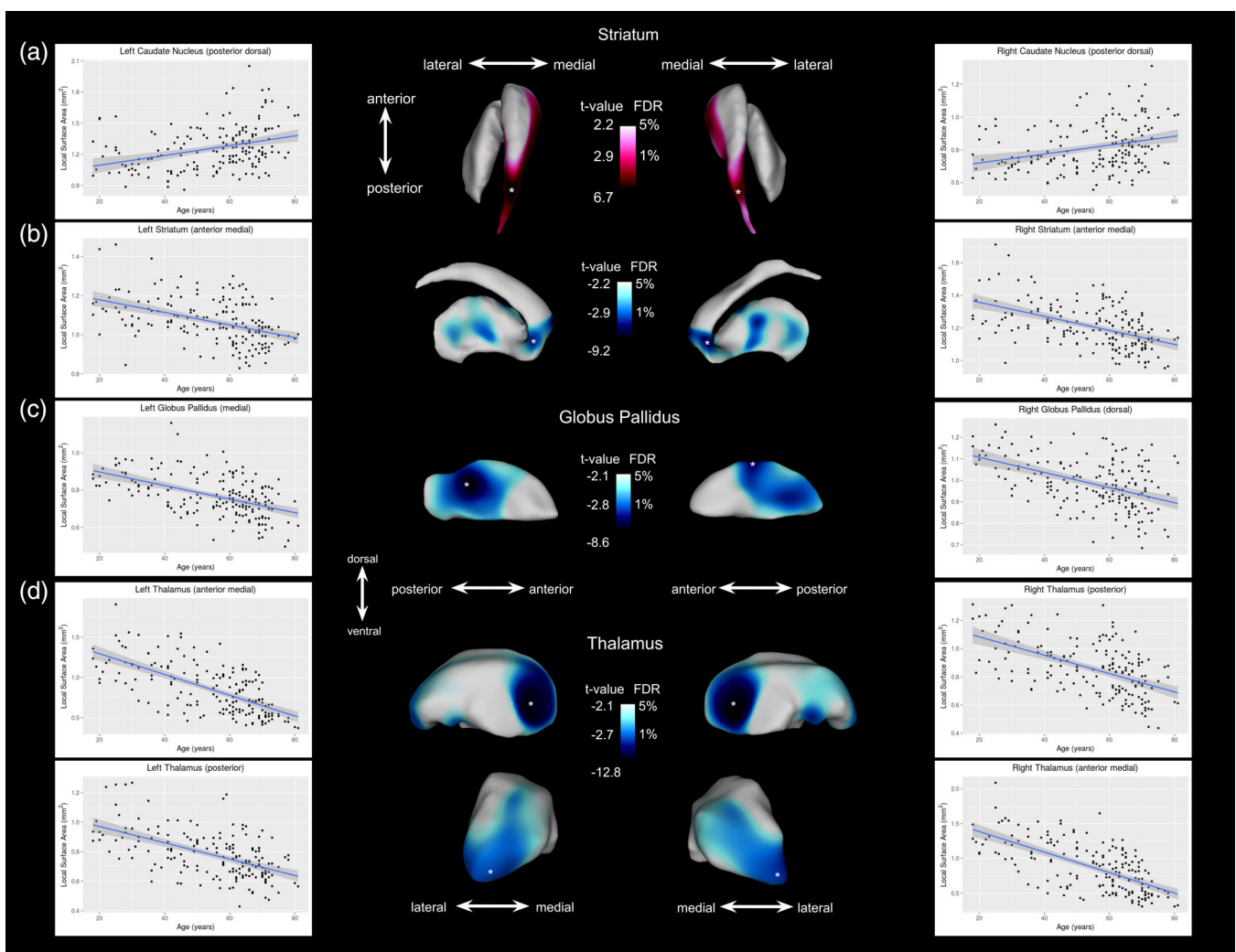


FIGURE 2 Age-related areal contraction and expansion in shape (surface area) observed at the 1% FDR threshold. Red color maps indicate local surface area expansion with age after 1–5% FDR correction; blue color maps on the subcortical surfaces indicate local surface area contraction with age after 1–5% FDR correction. Each plot displays the age versus surface area measurements for peak vertex (denoted by a white asterisk). (a) Age-related expansion in surface area of the bilateral anterior and dorsal posterior caudate nucleus. (b) Age-related contraction in surface area of the bilateral anterior and medial anterior striatum, particularly the anterior caudate nucleus and nucleus accumbens. (c) Age-related contraction was observed in the medial posterior end of the left and right globus pallidus. (d) Age-related contraction in surface area of the bilateral thalami, particularly in the anterior medial region and in the pulvinar nucleus (located at the posterior end of the thalamus)

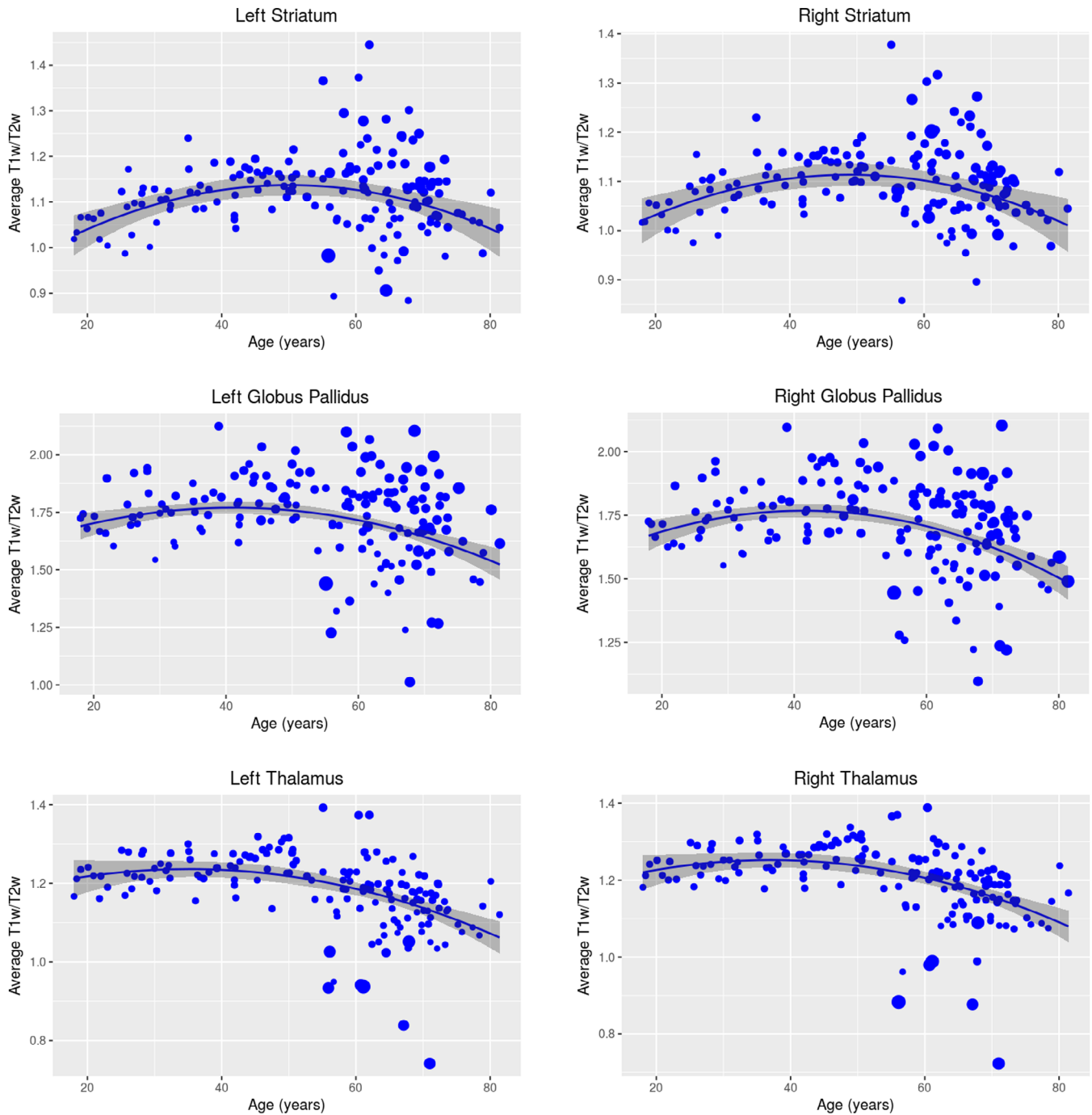


FIGURE 3 T1w/T2w-age relationships. Plots showing the relationship between age and average T1w/T2w for the striatum (left: $t = -4.35$, $p = 2.43e-5$; right: $t = -4.94$, $p = 1.95E-6$), globus pallidus (left: $t = -2.65$, $p = .00891$; right: $t = -3.33$, $p = .00109$), and thalamus (left: $t = -3.66$, $p = .000341$; right: $t = -3.95$, $p = .000116$), where the size of the points denotes the within-structure variance. The quadratic model was the best fit for all structures bilaterally, as determined by AIC. Quadratic age-related decline was observed for all structures of interest, where we observed an initial increase followed by a subsequent decline of average T1w/T2w, with a peak average T1w/T2w occurring at mid-life for all three structures bilaterally. The peak average T1w/T2w occurs at around 50 years old for the left and right striatum, whereas the peak occurs earlier, at around 45 years old, in the left and right globus pallidus and thalamus. After permutation testing, the quadratic model was no longer significant for the striatum [Color figure can be viewed at wileyonlinelibrary.com]

3.4 | Effect of years of education

The results do not significantly change when education is considered as a covariate in the statistical analyses. The only difference in

significance was for the T1w/T2w analyses of the striatum. After permutation testing, the left and the right striatum were no longer significant after permuting the model (left: $p = .11$; right: $p = .35$), whereas previously the left striatum was trending toward significance

TABLE 3 Impact of QC on the level of significance

		All subjects that passed motion QC (using manually corrected labels; <i>n</i> = 65)		Subjects that passed motion QC and original MAGeT QC (<i>n</i> = 47)		Subjects that passed motion QC and improved MAGeT QC (<i>n</i> = 53)	
		Left	Right	Left	Right	Left	Right
Volume	Striatum	***	**	<i>n.s.</i>	<i>n.s.</i>	*	<i>n.s.</i>
	Globus Pallidus	****	***	<i>n.s.</i>	<i>n.s.</i>	**	*
	Thalamus	****	****	<i>n.s.</i>	<i>n.s.</i>	**	**

n.s. $p > .05$; * $p \leq 0.05$; ** $p \leq .01$; *** $p \leq .001$; **** $p \leq .0001$.

TABLE 4 Impact of QC on the best fit model (as determined by AIC) for volume analyses

		All subjects that passed motion QC (using manually corrected labels; <i>n</i> = 65)		Subjects that passed motion QC and original MAGeT QC (<i>n</i> = 47)		Subjects that passed motion QC and improved MAGeT QC (<i>n</i> = 53)	
		Left	Right	Left	Right	Left	Right
Striatum	Linear	Linear	Linear	Linear	Linear	Quadratic	Linear
Globus Pallidus	Linear	Linear	Linear	Linear	Linear	Linear	Cubic
Thalamus	Cubic	Cubic	Cubic	Linear	Linear	Linear	Linear

($p = .0702$). See Supplementary Results section (Section 3.4, Figures S5–S7, and Table S2) for a detailed description of these results.

3.5 | Effect of sex

When sex was modeled as a covariate, the main effect of sex was not significant in any of the analyses performed. In analyses including an age by sex interaction, for the T1w/T2w analyses, the interaction was significant for the left and right globus pallidus (left: $t = -2.106$, $p = .0368$; right: $t = -2.033$, $p = .0438$), where the best fit age term model remained quadratic (as did when modeling sex as covariate in the model), however these results would not survive multiple comparisons correction. See Figure S8 for the age by sex relationship for average T1w/T2w for the globus pallidus. Moreover, for the surface area analyses, significant linear age by sex interactions (at FDR 15%) were observed in three regions of the left striatum (medial and dorsal caudate nucleus and the anterior part of the striatum), neither of the regions where significant age effect were observed (as shown in Figure 2). See Figure S8 for localized regions of the left striatum where a significant age by sex interaction was observed.

3.6 | Impact of QC on age trajectories

Table 3 demonstrates the impact of exclusion on the level of significance and Table 4 demonstrates the best fit model obtained for each segmentation method. Notably, the level of significance for the volume analyses is different among the three samples, such that the relationship between volume and age is no longer significant in the sample where many subjects were excluded due to inaccurate segmentation generated by the segmentation pipeline. Furthermore, the AIC-determined age–volume relationships for all of the subcortical

structures bilaterally were linear for this most stringently QC'ed sample, whereas different best-fits were observed when including more subjects when using segmentation technique that generated greater segmentation accuracy (manual segmentation and the improved version of MAGeT-Brain).

4 | DISCUSSION

This is the first report that simultaneously investigates subcortical volumes with corresponding local surface area measures and subcortical T1w/T2w using a healthy cohort of individuals spanning the entire adult lifespan (from ages 18 to 83). The results of this study support past evidence of differential aging of the striatum, globus pallidus, and thalamus across the adult lifespan in terms of morphology (i.e., volume, local surface area) and microstructure (i.e., T1w/T2w signal ratio). Differential subcortical volume–age relationships were observed across the entire adult lifespan when examining this cohort; we observed a negative linear volumetric relationship with age in the globus pallidus and a negative quadratic relationship with age in the thalamus. While the quadratic model was the best fit model for the striatum (as determined by AIC), the quadratic age term was not significant.

Complementary to the volume decline observed across the adult lifespan, local surface area contraction was observed for all three structures bilaterally, observed specifically in the posterior end of the globus pallidus and thalamus, and in the anterior regions of the striatum and thalamus, suggesting spatial specificity for the volumetric changes observed. Moreover, areal expansion was observed in the medial and dorsal posterior caudate nucleus region of the striatum. Average T1w/T2w was significantly different across the adult lifespan; a quadratic relationship was observed such that average

T1w/T2w gradually increased until about mid-age, then gradually declined thereafter, for all three structures of interest bilaterally, although the results for the striatum did not survive permutation testing.

Previous cross-sectional studies of adults have consistently identified decreases in volume of the basal ganglia and thalamus across the lifespan. Consistent with our findings, linear and quadratic decreases were reported for the basal ganglia and thalamus (Goodro et al., 2012; Greenberg et al., 2008; Gunning-Dixon et al., 1998; Inano et al., 2013; Raz et al., 2003; Sullivan et al., 2004; Van Der Werf et al., 2001). However, these studies report mixed results for the type of age relationship observed, with some studies finding linear decreases while others find nonlinear decreases or no change in subjects spanning approximately 20–90 years of age (Fjell et al., 2013; Goodro et al., 2012; Greenberg et al., 2008; Gunning-Dixon et al., 1998; Inano et al., 2013; Narvacan et al., 2017; Potvin et al., 2016; Raz et al., 2003; Sullivan et al., 2004; Van Der Werf et al., 2001; Walhovd et al., 2005, 2011). In particular, with regard to the striatum, inconsistencies in terms of trajectories are reported in the literature in part due to differences in its parcellation; some studies parse the striatum into the caudate nucleus, putamen, and nucleus accumbens (Cherubini et al., 2009; Goodro et al., 2012; Hagemeyer et al., 2013; Jäncke et al., 2015; Narvacan et al., 2017; Østby et al., 2009; Walhovd et al., 2005, 2011). Partial volume effects and lack of contrast between the subdivisions of the striatum (limited contrast to delineate the border between the caudate nucleus and nucleus accumbens, as well as defining the subdivision relative to the fine-scale cell bridges, known as striosomes, between the caudate and the putamen) were the main factors for investigating the striatum as a whole, as any attempt to subdivide the striatum is commonly based on heuristic definitions (Koo et al., 2006; Levitt et al., 2002; Yushkevich et al., 2006). While recent work has explored data-driven techniques to parcellate the striatum, for instance, using structural and/or functional connectivity, clustering techniques identify several clusters, parcellating the striatum beyond its traditional anatomic regions (caudate nucleus, putamen, and nucleus accumbens; Besson et al., 2017; Janssen, Jylänki, Kessels, & van Gerven, 2015; Pauli, O'Reilly, Yarkoni, & Wager, 2016). Beyond the variability in its delineation, we observe significant variability in the distribution of T1w/T2w values, particularly in older individuals (ages 55 and over; Figure 3). A possible reason for why this variability occurs in these individuals, and consequently perhaps why the quadratic T1w/T2w age relationship did not survive permutation testing, is the increased variability typically observed in older individuals, as motor dysfunction, cognitive decline, and the prevalence of geriatric depression have been associated with age (Ardila, Ostrosky-Solis, Rosselli, & Gómez, 2000; Bartzokis, Lu, & Mintz, 2004; Deary et al., 2009; Seidler et al., 2010; Volkow et al., 1998). However, the thalamus has also been associated with motor and cognitive dysfunctions in aging and neurodegeneration (Halliday, 2009; Tang et al., 2014) yet there is seemingly less variability with the T1w/T2w values obtained for the thalamus in older individuals (compared to the values obtained for the striatum of these individuals; see Figure 3). While the dorsal/ventral dichotomy observed with respect to surface area and

age (with an areal contraction in more dorsal regions and an areal expansion in more ventral regions) could account for some of this variability (especially given the nature of an averaged T1w/T2w value), the biological underpinnings for this variability occurring with the striatum remain to be elucidated.

4.1 | Possible biological and functional correlates

While MR-based measures cannot provide insight to the underlying biological mechanisms of the findings observed across the adult lifespan, nonetheless, age-related volumetric decline has previously been hypothesized to be the result of loss of neuronal bodies, decreases in dendritic arborization, synaptic pruning, refinement of circuits, and/or loss of connections (Gunning-Dixon et al., 1998; Narvacan et al., 2017; Østby et al., 2009; Pfefferbaum et al., 2013; Raz et al., 2003; Raz & Rodrigue, 2006; Tamnes et al., 2013; Ziegler et al., 2012). However, it should be noted that the underlying cellular mechanisms driving volume reductions may be influenced by physiological mechanisms unique to each structure (Narvacan et al., 2017). For example, iron accumulation in the brain has been shown to predict putamen but not caudate volume decline in late life (Daugherty & Raz, 2016). In other words, further work examining these cellular mechanisms is crucial to understanding the potential sources underlying the relationship between age and morphology observed across the adult lifespan.

In addition to volume decline across the age span, we observed local surface area contraction in the posterior parts of the globus pallidus and thalamus, and in the anterior parts of the striatum and thalamus. These findings are of particular relevance given that these morphological findings, the volumetric decline with surface area contraction of these regions of the basal ganglia and thalamus, are in accordance with other age-related findings reported in the literature. Particularly, the posterior regions of these basal ganglia nuclei, specifically the globus pallidus as well as the ventral posterior regions of the thalamus, are known to be involved in motor functions, given their indirect and direct respective projections to the sensorimotor cortical areas (Parent, 1990), functions that have been reported to decline with age (Ardila et al., 2000; Bartzokis et al., 2004; Deary et al., 2009; Seidler et al., 2010; Volkow et al., 1998). Moreover, the anterior striatum is known to be involved in associative and limbic functioning (Parent, 1990); notably, the head of the caudate nucleus and the nucleus accumbens are subregions of the anterior striatum that are implicated in cognitive functioning and have also been previously reported to decline with age (Ardila et al., 2000; Bartzokis et al., 2004; Deary et al., 2009; Seidler et al., 2010; Volkow et al., 1998). Furthermore, the pulvinar nucleus of the thalamus projects to the parietal and temporal association cortices, which are known to be affected in disorders of pathological aging, such as in Alzheimer's and Parkinson's disease (Braak et al., 2003; Braak & Braak, 1995).

In addition to surface area contraction and volumetric decline with age, we also observe an expansion of the local surface area of the medial and dorsal posterior regions of the caudate nucleus occurring with age, which are primarily involved in associative functioning, with

some involvement in sensorimotor functioning from the anterior end of the medial caudate nucleus. However, it should be noted that the area in which the expansion is observed lies adjacent to the lateral ventricles. Given that ventricle size is known to increase with age, it is entirely possible that expansions in the ventricles could be influencing this finding. Nonetheless, despite an expansion in surface area in these dorsal regions of the striatum, we report an overall decline in global structure volume with age, which may be in part due to a greater surface area contraction occurring in the ventral part of the striatum.

Given that the focus of MR-based investigations of subcortical structure have primarily focused on volumetry, the examination of other anatomically based morphological measures is crucial in parsing the heterogeneity of the findings reported in the aging literature, particularly for the basal ganglia. Of note, volumetric measurements of the basal ganglia in adults present a unique challenge in that the striatum and globus pallidus accumulate more iron than most other subcortical brain regions, with the iron concentration being especially high in the globus pallidus (Bartzokis et al., 2000; Hallgren & Sourander, 1958; Raz et al., 2003). The microstructural profile of these structures can influence their MR-derived volumes, such that the presence of iron deposits can render the MR-based volumetric measures insensitive to age-related shrinkage; this phenomenon reflects a prevalent factor that has rarely been acknowledged as a confounding factor among existing volumetric aging studies (Raz et al., 2003). Thus, beyond subcortical morphology, we examined a marker of age-modulated microstructural changes in these deep gray matter structures using the T1w/T2w signal ratio across the adult lifespan. Loss of myelin, decreased nodes of Ranvier density, deformation of myelin sheaths, increased presence of iron, and other microstructural damage are known to occur with age (Arshad, Stanley, & Raz, 2016; Cherubini et al., 2009; Haacke et al., 2005; Péran et al., 2007; Peters, 2002; Tang, Nyengaard, Pakkenberg, & Gundersen, 1997).

A major finding of this study is the quadratic relationship observed between age and average T1w/T2w, where peak T1w/T2w occurs at around 45–50 years old for these subcortical structures. These results are in congruence with studies investigating age-effects on nerve fibers, myelinated axons that provide rapid and efficient transfer of information between different brain regions and to the periphery. Previous postmortem studies have reported a protracted myelination of subcortical myelin into the middle age, followed by a gradual decline in the late adulthood (Benes, Turtle, Khan, & Farol, 1994; Marnier, Nyengaard, Tang, & Pakkenberg, 2003; Peters, 2002). Work by Marnier et al. (2003), in which a stereologic method was used to estimate the total volume, total length, and the diameter of myelinated nerve fibers in autopsied brains, reported substantial loss of white matter fibers with age, and proposed that this biological mechanism is the main source of cognitive decline reported in older individuals. Beyond cognition, subcortical myelin may play a critical role in the maturation of emotional processes. Benes et al. (1994) reported a negative quadratic relationship between hippocampal myelin and age using postmortem data in healthy individuals across the adult lifespan, and argued that while cognitive functioning is fully developed around the

early stage of adulthood, emotional intelligence such as anxiety, sociability, and affect intensity is thought to continue to develop through the midlife period, and may be a reason for the peak occurring at middle-age. Given the role of the basal ganglia in emotional and behavioral functioning (Jahanshahi et al., 2015), the same can be said for these subcortical structures, such that middle-age maturation of limbic functions based on increased life experiences could be associated with peak in T1w/T2w occurring at middle-age in the striatum, globus pallidus, and thalamus. Research in emotional aging suggests that emotional experiences become more stable with advancing age (Benes et al., 1994; Carstensen et al., 2011; Diener, Sandvik, & Larsen, 1985; Eysenck, MacLeod, & Mathews, 1987; Scheibe & Carstensen, 2010). Specifically, studies have reported decreased anxiety, sociability, and affect intensity occurring through the midlife period (Diener et al., 1985; Eysenck et al., 1987), high levels of affective well-being and emotional stability at around the age of 70 (Scheibe & Carstensen, 2010), as well as a decline in the frequency of negative emotions until approximately 60 years old, which ceases thereafter, following a quadratic relationship (Carstensen, Pasupathi, Mayr, & Nesselrode, 2000). It would be interesting to relate the neuroimaging measures used here to relate emotional aging indices in future work.

Moreover, non-postmortem studies investigating *in vivo* assessment of cortical and subcortical myelin using MRI techniques have also reported a quadratic inverted U relationship between age and myelin (Arshad et al., 2016; Bartzokis et al., 2004; Grydeland et al., 2013). Although T1w/T2w signal ratio in cortical and subcortical structures is not directly comparable because the microstructural changes with aging are different and will contribute differently to the MRI signal (e.g., iron deposition is higher in the subcortex, particularly in these structures), two recent studies examining the effects of aging using the T1w/T2w signal ratio technique both reported similar age relationships. Grydeland et al. (2013) investigated cortical T1w/T2w in individuals aged 8–83 years old and reported that intracortical myelin increased linearly until the late 30s, followed by 20 stable years before declining as of the late 50s. Similarly, Shafee et al. (2015) investigated cortical T1w/T2w in individuals aged 18–35 years old and reported a linear increase of T1w/T2w myelin with age, with no detectable quadratic age effect, replicating the increase in cortical T1w/T2w in individuals aged 18–35 previously observed by Grydeland et al. (2013). Given these reciprocal connections between subcortical structures and the cerebral cortex, the agreement between the age–T1w/T2w relationships observed in the cortex and subcortex could suggest a possible common biological mechanism driving these relationships observed across the adult lifespan.

The assessment of subcortical microstructure may help to understand the differential effects of age on volume, and can provide insight into the functional deficits that are known to occur with age. Given the role of the basal ganglia and thalamus as important network hubs and relays, the investigation of myelinated axonal fibers terminating in these structures is of particular relevance given the role of myelin in high-speed transmission and synchronization for the execution of cognitive and motor functions, which are known to decline with age (Ardila et al., 2000; Bartzokis et al., 2004; Deary et al., 2009;

Seidler et al., 2010; Volkow et al., 1998). Unfortunately, subcortical gray matter myelin has largely been neglected in the aging literature, despite being an important feature in mediating everyday functioning, largely due to limitations of *in vivo* analyses of myelin. In fact, studies in which investigate “subcortical myelin” fall into two main categories: (a) myelin of subcortical white matter tracts, which are most commonly examined and (b) myelin of the subcortical structures, which few studies have examined. These two research domains of subcortical myelin stem from two MR-based techniques that are used to examine myelin; diffusion tensor imaging (DTI), particularly fractional anisotropy (FA), and radial diffusivity (RD), and quantitative techniques, such as magnetization transfer ratio, and T1 and T2 relaxation maps, respectively. As a result, to date, life-span age differences in subcortical myelination have been inferred predominantly from DTI-based indices, where multiple cross-sectional studies have reported significant negative associations between age and FA as well as positive associations between age and RD of subcortical myelin (Abe et al., 2008; Cherubini et al., 2009; Lebel, Walker, Leemans, Phillips, & Beaulieu, 2008; Lebel et al., 2012; Madden et al., 2012; Wang et al., 2010); however is also unclear whether higher order models were examined. DTI achieves its sensitivity to myelin through its sensitivity to the diffusion magnitude and direction of water molecules, such that new or thicker myelin reduces the inter-axonal space and thus increases the anisotropy of water diffusion (Feldman et al., 2010). However, the diffusivity of water is influenced by numerous other factors that are independent of myelin, including axonal packing density, intra-voxel orientational dispersion, membrane permeability, oligodendrocyte proliferation, and tissue water content (Jones et al., 2013; Mädler et al., 2008). Moreover, the results of cross-sectional studies examining age differences using FA and RD are inconsistent and differ from the patterns of lifespan myelination suggested by the postmortem studies (Arshad et al., 2016). Thus, DTI-based descriptors of the white matter diffusion properties do not specifically reflect myelin content, and are likely better suited to examine the state of the white matter (Arshad et al., 2016; Jones et al., 2013).

With this, the literature has shifted toward using other techniques to examine myelin. Specifically, with recent advances and increasing availability of quantitative MRI acquisition techniques, researchers are beginning to examine myelin using more direct measurements of microstructure, such as myelin. Quantitative MRI techniques to measure myelin have primarily consisted of T1 relaxation time and magnetization transfer ratio (MTR) maps, as well as T2 relaxation techniques that separate the MR signal to obtain an indirect measure of myelin. However, these quantitative techniques have also been shown to be influenced by other underlying biological processes (e.g., inflammation) that contribute to the myelin MRI signal obtained (Laule et al., 2007). One prominent technique is myelin water imaging (MWI), which exploits the different T2-relaxation times of water trapped between myelin sheaths, yielding a myelin water fraction (MWF) parameter (MacKay et al., 1994; Uddin et al., 2018). The accuracy of MWI has been validated in studies correlating histopathological myelin samples and neuroimaging-derived MWF in animal (Beaulieu et al., 1998; Garreau et al., 2000; Odobina et al., 2005; Stanisiz et al., 2004; Webb et al.,

2003) and human studies (Laule et al., 2006, 2008). So far, only few studies used MWI to study healthy myelin maturation. However, there is still inconsistency between studies in terms of the nature of the myelin–age relationships, where some studies also report a linear decline with age for these quantitative metrics (Callaghan et al., 2014; Cherubini et al., 2009), while other studies have observed quadratic associations between age and myelin, with peak myelin varying between 30 and 50 years of age (Arshad et al., 2016; Ge et al., 2002; Inglese & Ge, 2004; Watanabe et al., 2013; Yeatman et al., 2014).

Beyond these two methods, based on data availability, we have chosen to use the ratio of the signal intensities of T1w and T2w images in the current study as a measure of myelin. Our findings are supported by the correspondence between cortical patterns of T1w/T2w and myelin (Glasser et al., 2016; Glasser & Van Essen, 2011). Further, the T1w/T2w ratio technique has been used to map the myelin content of the cerebral cortex (Glasser & Van Essen, 2011), and to study the effects of aging (Grydeland et al., 2013; Lee et al., 2015; Shafee et al., 2015) and disease (Ganzetti, Wenderoth, & Mantini, 2015; Ishida et al., 2017; Iwatani et al., 2015). However, to date, there have been no investigations of subcortical T1w/T2w in healthy adults across the adult lifespan.

4.2 | Methodological considerations and limitations

The findings reported here should be viewed in the context of the following methodological limitations. One drawback of MR imaging is the inability to identify the cellular mechanisms underlying the MR-derived measures. Further work using a combination of histology and imaging would provide a superior, cohesive understanding of the volume, surface area, and T1w/T2w–age relationships reported. Nonetheless, MRI is beneficial, as it allows us to investigate structural age-related brain changes *in vivo*, and is crucial for establishing trajectories of development and degeneration across the human lifespan.

As with all MR-based studies, motion is a big obstacle given its ability to drastically reduce sample sizes; however, this exclusion is a necessity as it has been shown that motion changes the information content of the images in the direction we would typically expect in an atrophy study (Lerch et al., 2017), where more motion induces an apparent reduction in gray matter that is difficult to distinguish from true atrophy (Reuter et al., 2015). However, by excluding participants with motion present in their images, the results are biased toward younger individuals as motion is nonrandomly distributed with respect to age (e.g., children move more than adults and elderly subjects move more than middle aged subjects; Pardoe, Hiess, & Kuzniecky, 2016). While we cannot control the bias of exclusion due to motion, excluding individuals for inaccurate segmentation, particularly due to the presence of neuroanatomical variation, is a bias that can and should be reduced given that this exclusion biases the results once again toward younger individuals, as well as individuals with average and smaller than average ventricle size, and without white matter hyperintensities, which is not an accurate representation of the population of interest, given that these neuroanatomical features occur normally with age.

In this work, we used the T1w/T2w signal ratio technique to complement the morphological analyses performed (volume and surface area) with the aim of using this metric as a measure of tissue microstructure, particularly that of myelin based on previous work that demonstrated correspondence between cortical patterns of T1w/T2w and myelin (Glasser et al., 2016; Glasser & Van Essen, 2011). However, we acknowledge the contribution of other nonmyelin biological factors to the MR signal obtained from T1w and T2w MR images. Recent work has reported that the T1 signal is also sensitive to macromolecules (e.g., the proteins and lipids forming cellular membranes), water content of brain tissues, and to a lesser extent iron, and the T2 signal is sensitive to iron and deoxyhemoglobin content, in addition to myelin (Tardif et al., 2016). Most notably, myelin and inflammation both alter the signal intensity of T1w and T2w images in opposite directions, both contributing to an increase in T1w/T2w ratio values. Resultantly, it has been suggested T1w/T2w is a less than optimal index of white matter myelin (Arshad et al., 2016; Uddin et al., 2018). However, while Uddin et al. (2018) cite low correlations between T1w/T2w and a histologically validated technique for examining myelin, myelin water fraction (MWF), for white matter structures, they nonetheless cite moderate correlations for subcortical gray matter structures (Uddin et al., 2018, 2019). Thus, a conservative approach for using the T1w/T2w signal ratio is its use as a nonspecific biomarker of microstructure, with the use of quantitative MRI techniques, such as magnetization transfer or myelin water imaging, to parse out the effect of differential elements of the microstructure, such as myelin using MWI and iron using R2* (the short spin-spin T2 relaxation; Péran et al., 2007; Stüber et al., 2014).

A final consideration of the results reported for the T1w/T2w analyses is the different scan acquisition parameters for the T2w images acquired for the HA and ADB study. While the effect of reducing the scan time acquisition on the T2w signal is not known, the averaging of two T2w images does increase the signal-to-noise ratio, which can have an impact on the T1w/T2w analyses. While we attempted to account any possible difference that may result from the two T2w acquisitions protocols (from the HA and ADB study) by modeling scan acquisition as a random effect for the T1w/T2w analyses, this difference in combination with the difference in the subject demographics between the HA and ADB study, particularly age (that is, participants in the ADB study are older than those in the HA study), could introduce more variability. Thus, future work using a single cohort of healthy individuals spanning the adult lifespan would reduce these sources of variability. Moreover, it could provide insight as to whether the T2w acquisition difference is a legitimate concern, and whether mixed effects modeling mitigates any differences. Nonetheless, when examining the T1w/T2w analyses for the HA study cohort only ($n = 87$), which spans the entire adult lifespan (ages 18–80), the quadratic relationship still holds (as determined by AIC and permutation testing); see Figure S9 for T1w/T2w versus age plots for the HA study cohort. The consistency of these results quells any concerns for cohort-dependent difference and the possible consequences of different signal-to-noise ratio for the T2w images (as a result of a different scan acquisition protocol and the averaging of two T2w images

acquired for each subject). By adding additional subjects, from the ADB study ($n = 75$), to the HA study cohort, as a way of increasing sample size ($N = 162$), the quadratic T1w–T2w age relationship is reinforced.

5 | CONCLUSION

To the best of our knowledge, this study is the first MRI study to report simultaneous measurements of subcortical volume, surface area, and T1w/T2w signal ratio in the striatum, globus pallidus, and thalamus using structural MR images in individuals across the entire adult lifespan (in healthy individuals aged 18–83). This study demonstrates differential subcortical volume across the entire adult lifespan, with linear age relationships observed for the globus pallidus, and a quadratic relationship observed for the striatum and thalamus. Along with an age-related decline in volume, we observed complementary local surface area contraction in all three structures bilaterally, and surface area expansion in the striatum across the adult lifespan. Furthermore, average T1w/T2w was significantly different across the adult lifespan; average T1w/T2w gradually increased until about mid-age, followed by a gradual decline thereafter for all three structures of interest bilaterally, with peak T1w/T2w occurring at around 45–50 years old. The age-dependent relationship of subcortical T1w/T2w signal ratio observed across the adult lifespan may provide important insights on the maturation of behavioral processes in which these structures are implicated, and that continue to develop until mid-age, reflecting the peak T1w/T2w attainment observed at mid-life in these subcortical structures. Moreover, this quadratic relationship may also provide insight on the role of microstructure in disorders in which these subcortical structures are implicated and compromised. However, both the volume and T1w/T2w age relationships observed for the striatum do not survive permutation testing. In conclusion, our results provide normative baseline data of normal aging, which may consequently aid in the interpretation of data collected from patients with neuropsychiatric and neurodegenerative conditions.

ACKNOWLEDGMENTS

ST received funding from the Natural Sciences and Engineering Research Council and the Fonds de la Recherche en Santé du Québec. MMC is supported by the Fonds de Recherches Santé Québec, Canadian Institutes of Health Research, National Sciences and Engineering Research Council of Canada, Weston Brain Institute, Alzheimer's Society, Brain Canada, and the Michael J. Fox Foundation for Parkinson's Research. GAD is supported in part by funding provided by Brain Canada, in partnership with Health Canada, for the Canadian Open Neuroscience Platform initiative. The High-resolution memory-circuit and microstructural magnetic resonance imaging-based biomarkers for identifying risk for Alzheimer's disease, also known as the Alzheimer's Disease Biomarker (ADB) Study was supported by the Weston Brain Institute. Part of the data used in preparation of this article were obtained from the Pre-symptomatic Evaluation of Novel

or Experimental Treatments for Alzheimer's Disease (PREVENT-AD) program (<http://www.douglas.qc.ca/page/prevent-alzheimer>) at the Douglas Mental Health University Institute, as part of the ADB study.

CONFLICT OF INTEREST

The authors have no conflict of interest to declare.

DATA AVAILABILITY STATEMENT

The data that support the findings of this study are available on request from the senior author [MMC]. The data are not publicly available due to privacy or ethical restrictions.

ORCID

Stephanie Tullo  <https://orcid.org/0000-0003-4608-3000>

Gabriel A. Devenyi  <https://orcid.org/0000-0002-7766-1187>

Christine L. Tardif  <https://orcid.org/0000-0001-8356-6808>

REFERENCES

- Abe, O., Yamasue, H., Aoki, S., Suga, M., Yamada, H., Kasai, K., ... & Ohtomo, K. (2008). Aging in the CNS: comparison of gray/white matter volume and diffusion tensor data. *Neurobiology of aging*, 29(1), 102–116. <https://doi.org/10.1016/j.neurobiolaging.2006.09.003>
- Abedelahi, A., Hasanzadeh, H., Hadizadeh, H., & Joghataie, M. T. (2013). Morphometric and volumetric study of caudate and putamen nuclei in normal individuals by MRI: Effect of normal aging, gender and hemispheric differences. *Polish Journal of Radiology*, 78(3), 7. <https://doi.org/10.12659/PJR.889364>
- Abi-Dargham, A., & Meyer, J. M. (2014). Schizophrenia: The role of dopamine and glutamate. *The Journal of Clinical Psychiatry*, 75(3), 274–275. <https://doi.org/10.4088/JCP.13078co7c>
- Akaike, H. (1974). A new look at the statistical model identification. *IEEE Transactions on Automatic Control*, 19(6), 716–723. <https://doi.org/10.1109/TAC.1974.1100705>
- Alexander, G. E., DeLong, M. R., & Strick, P. L. (1986). Parallel organization of functionally segregated circuits linking basal ganglia and cortex. *Annual Review of Neuroscience*, 9(1), 357–381. <https://doi.org/10.1146/annurev.ne.09.030186.002041>
- Ardila, A., Ostrosky-Solis, F., Rosselli, M., & Gómez, C. (2000). Age-related cognitive decline during normal aging: The complex effect of education. *Archives of Clinical Neuropsychology*, 15(6), 495–513.
- Arshad, M., Stanley, J. A., & Raz, N. (2016). Adult age differences in subcortical myelin content are consistent with protracted myelination and unrelated to diffusion tensor imaging indices. *NeuroImage*, 143, 26–39. <https://doi.org/10.1016/j.neuroimage.2016.08.047>
- Aylward, E. H., Li, Q., Stine, O. C., Ranen, N., Sherr, M., Barta, P. E., ... Ross, C. A. (1997). Longitudinal change in basal ganglia volume in patients with Huntington's disease. *Neurology*, 48(2), 394–399.
- Backhausen, L. L., Herting, M. M., Buse, J., Roessner, V., Smolka, M. N., & Vetter, N. C. (2016). Quality control of structural MRI images applied using FreeSurfer—A hands-on workflow to rate motion artifacts. *Frontiers in Neuroscience*, 10, 558. <https://doi.org/10.3389/fnins.2016.00558>
- Bartzokis, G., Lu, P. H., & Mintz, J. (2004). Quantifying age-related myelin breakdown with MRI: Novel therapeutic targets for preventing cognitive decline and Alzheimer's disease. *Journal of Alzheimer's Disease*, 6(s6), S53–S59.
- Bartzokis, G., Sultzer, D., Cummings, J., Holt, L. E., Hance, D. B., Henderson, V. W., & Mintz, J. (2000). In vivo evaluation of brain iron in Alzheimer disease using magnetic resonance imaging. *Archives of General Psychiatry*, 57(1), 47–53. <https://doi.org/10.1001/archpsyc.57.1.47>
- Beaulieu, C., Fenrich, F. R., & Allen, P. S. (1998). Multicomponent water proton transverse relaxation and T2-discriminated water diffusion in myelinated and nonmyelinated nerve. *Magnetic resonance imaging*, 16(10), 1201–1210. [https://doi.org/10.1016/S0730-725X\(98\)00151-9](https://doi.org/10.1016/S0730-725X(98)00151-9)
- Bedford, S. A., Park, M. T. M., Devenyi, G. A., Tullo, S., Germann, J., Patel, R., ... Craig, M. C. (2019). Large-scale analyses of the relationship between sex, age and intelligence quotient heterogeneity and cortical morphometry in autism spectrum disorder. *Molecular Psychiatry*, 1, 1–15. <https://doi.org/10.1038/s41380-019-0420-6>
- Belin, D., Jonkman, S., Dickinson, A., Robbins, T. W., & Everitt, B. J. (2009). Parallel and interactive learning processes within the basal ganglia: Relevance for the understanding of addiction. *Behavioural Brain Research*, 199(1), 89–102. <https://doi.org/10.1016/j.bbr.2008.09.027>
- Benes, F. M., Turtle, M., Khan, Y., & Farol, P. (1994). Myelination of a key relay zone in the hippocampal formation occurs in the human brain during childhood, adolescence, and adulthood. *Archives of General Psychiatry*, 51(6), 477–484.
- Benjamini, Y., & Hochberg, Y. (1995). Controlling the false discovery rate: A practical and powerful approach to multiple testing. *Journal of the Royal Statistical Society: Series B: Methodological*, 57, 289–300.
- Bernal-Rusiel, J. L., Greve, D. N., Reuter, M., Fischl, B., Sabuncu, M. R., & Alzheimer's Disease Neuroimaging Initiative. (2013). Statistical analysis of longitudinal neuroimage data with linear mixed effects models. *NeuroImage*, 66, 249–260. <https://doi.org/10.1016/j.neuroimage.2012.10.065>
- Besson, P., Carrière, N., Bandt, S. K., Tommasi, M., Leclerc, X., Derambure, P., ... Tyvaert, L. (2017). Whole-brain high-resolution structural connectome: Inter-subject validation and application to the anatomical segmentation of the striatum. *Brain Topography*, 30(3), 291–302. <https://doi.org/10.1007/s10548-017-0548-0>
- Braak, H., & Braak, E. V. A. (1995). Staging of Alzheimer's disease-related neurofibrillary changes. *Neurobiology of Aging*, 16(3), 271–278.
- Braak, H., Del Tredici, K., Rüb, U., De Vos, R. A., Steur, E. N. J., & Braak, E. (2003). Staging of brain pathology related to sporadic Parkinson's disease. *Neurobiology of Aging*, 24(2), 197–211.
- Brain Development Cooperative Group. (2012). Total and regional brain volumes in a population-based normative sample from 4 to 18 years: The NIH MRI study of Normal brain development. *Cerebral Cortex*, 22(1), 1–12. <https://doi.org/10.1093/cercor/bhr018>
- Callaghan, M. F., Freund, P., Draganski, B., Anderson, E., Cappelletti, M., Chowdhury, R., ... Lutti, A. (2014). Widespread age-related differences in the human brain microstructure revealed by quantitative magnetic resonance imaging. *Neurobiology of Aging*, 35(8), 1862–1872. <https://doi.org/10.1016/j.neurobiolaging.2014.02.008>
- Carstensen, L. L., Pasupathi, M., Mayr, U., & Nesselroade, J. R. (2000). Emotional experience in everyday life across the adult life span. *Journal of Personality and Social Psychology*, 79(4), 644. <https://doi.org/10.1037/0022-3514.79.4.644>
- Carstensen, L. L., Turan, B., Scheibe, S., Ram, N., Ersner-Hershfield, H., Samanez-Larkin, G. R., ... Nesselroade, J. R. (2011). Emotional experience improves with age: Evidence based on over 10 years of experience sampling. *Psychology and Aging*, 26(1), 21. <https://doi.org/10.1037/a0021285>
- Chakravarty, M. M., Bertrand, G., Hodge, C. P., Sadikot, A. F., & Collins, D. L. (2006). The creation of a brain atlas for image guided neurosurgery using serial histological data. *NeuroImage*, 30(2), 359–376. <https://doi.org/10.1016/j.neuroimage.2005.09.041>
- Chakravarty, M. M., Rapoport, J. L., Giedd, J. N., Raznahan, A., Shaw, P., Collins, D. L., ... Gogtay, N. (2015). Striatal shape abnormalities as novel neurodevelopmental endophenotypes in schizophrenia: A

- longitudinal study. *Human Brain Mapping*, 36(4), 1458–1469. <https://doi.org/10.1002/hbm.22715>
- Chakravarty, M. M., Sadikot, A. F., Germann, J., Bertrand, G., & Collins, D. L. (2008). Towards a validation of atlas warping techniques. *Medical Image Analysis*, 12(6), 713–726. <https://doi.org/10.1016/j.media.2008.04.003>
- Chakravarty, M. M., Sadikot, A. F., Germann, J., Hellier, P., Bertrand, G., & Collins, D. L. (2009). Comparison of piece-wise linear, linear, and nonlinear atlas-to-patient warping techniques: Analysis of the labeling of subcortical nuclei for functional neurosurgical applications. *Human Brain Mapping*, 30(11), 3574–3595. <https://doi.org/10.1002/hbm.20780>
- Chakravarty, M. M., Steadman, P., van Eede, M. C., Calcott, R. D., Gu, V., Shaw, P., ... Lerch, J. P. (2013). Performing label-fusion-based segmentation using multiple automatically generated templates. *Human Brain Mapping*, 34(10), 2635–2654. <https://doi.org/10.1002/hbm.22092>
- Cherubini, A., Péran, P., Caltagirone, C., Sabatini, U., & Spalletta, G. (2009). Aging of subcortical nuclei: Microstructural, mineralization and atrophy modifications measured in vivo using MRI. *NeuroImage*, 48(1), 29–36. <https://doi.org/10.1016/j.neuroimage.2009.06.035>
- Coffey, C. E., Lucke, J. F., Saxton, J. A., Ratcliff, G., Unitas, L. J., Billig, B., & Bryan, R. N. (1998). Sex differences in brain aging: A quantitative magnetic resonance imaging study. *Archives of Neurology*, 55(2), 169–179.
- Collins, D. L., Neelin, P., Peters, T. M., & Evans, A. C. (1994). Automatic 3D intersubject registration of MR volumetric data in standardized Talairach space. *Journal of Computer Assisted Tomography*, 18(2), 192–205.
- Courchesne, E., Chisum, H. J., Townsend, J., Cowles, A., Covington, J., Egaas, B., ... Press, G. A. (2000). Normal brain development and aging: Quantitative analysis at in vivo MR imaging in healthy volunteers. *Radiology*, 216(3), 672–682. <https://doi.org/10.1148/radiology.216.3.r00au37672>
- Daugherty, A. M., & Raz, N. (2016). Accumulation of iron in the putamen predicts its shrinkage in healthy older adults: A multi-occasion longitudinal study. *NeuroImage*, 128, 11–20. <https://doi.org/10.1016/j.neuroimage.2015.12.045>
- Deary, I. J., Corley, J., Gow, A. J., Harris, S. E., Houlihan, L. M., Marioni, R. E., ... Starr, J. M. (2009). Age-associated cognitive decline. *British Medical Bulletin*, 92(1), 135–152. <https://doi.org/10.1093/bmb/ldp033>
- Diener, E., Sandvik, E., & Larsen, R. J. (1985). Age and sex effects for emotional intensity. *Developmental Psychology*, 21(3), 542. <https://doi.org/10.1037/0012-1649.21.3.542>
- Ducharme, S., Albaugh, M. D., Nguyen, T. V., Hudziak, J. J., Mateos-Pérez, J. M., Labbe, A., ... Brain Development Cooperative Group. (2016). Trajectories of cortical thickness maturation in normal brain development—The importance of quality control procedures. *NeuroImage*, 125, 267–279. <https://doi.org/10.1016/j.neuroimage.2015.10.010>
- Eskildsen, S. F., Coupé, P., Fonov, V., Manjón, J. V., Leung, K. K., Guizard, N., ... Alzheimer's Disease Neuroimaging Initiative. (2012). BEaST: Brain extraction based on nonlocal segmentation technique. *NeuroImage*, 59(3), 2362–2373. <https://doi.org/10.1016/j.neuroimage.2011.09.012>
- Eysenck, M. W., MacLeod, C., & Mathews, A. (1987). Cognitive functioning and anxiety. *Psychological Research*, 49(2–3), 189–195. <https://doi.org/10.1007/BF00308686>
- Feinberg, D. A., Hale, J. D., Watts, J. C., Kaufman, L., & Mark, A. (1986). Halving MR imaging time by conjugation: Demonstration at 3.5 kG. *Radiology*, 161(2), 527–531. <https://doi.org/10.1148/radiology.161.2.3763926>
- Feldman, H. M., Yeatman, J. D., Lee, E. S., Barde, L. H., & Gaman-Bean, S. (2010). Diffusion tensor imaging: a review for pediatric researchers and clinicians. *Journal of developmental and behavioral pediatrics: JDBP*, 31(4), 346. <https://doi.org/10.1097/DBP.0b013e3181dcaab8>
- Fennema-Notestine, C., Gamst, A. C., Quinn, B. T., Pacheco, J., Jernigan, T. L., Thal, L., ... Fischl, B. (2007). Feasibility of multi-site clinical structural neuroimaging studies of aging using legacy data. *Neuroinformatics*, 5(4), 235–245. <https://doi.org/10.1007/s12021-007-9003-9>
- Fischl, B., Salat, D. H., Busa, E., Albert, M., Dieterich, M., Haselgrove, C., ... Montillo, A. (2002). Whole brain segmentation: Automated labeling of neuroanatomical structures in the human brain. *Neuron*, 33(3), 341–355.
- Fjell, A. M., Westlye, L. T., Amlie, I., Espeseth, T., Reinvang, I., Raz, N., ... Dale, A. M. (2009). Minute effects of sex on the aging brain: A multi-sample magnetic resonance imaging study of healthy aging and Alzheimer's disease. *Journal of Neuroscience*, 29(27), 8774–8783. <https://doi.org/10.1523/JNEUROSCI.0115-09.2009>
- Fjell, A. M., Westlye, L. T., Grydeland, H., Amlie, I., Espeseth, T., Reinvang, I., ... Alzheimer Disease Neuroimaging Initiative. (2013). Critical ages in the life course of the adult brain: Nonlinear subcortical aging. *Neurobiology of Aging*, 34(10), 2239–2247. <https://doi.org/10.1016/j.neurobiolaging.2013.04.006>
- Fotos, A. F., Mintun, M. A., Snyder, A. Z., Morris, J. C., & Buckner, R. L. (2008). Brain volume decline in aging: Evidence for a relation between socioeconomic status, preclinical Alzheimer disease, and reserve. *Archives of Neurology*, 65(1), 113–120. <https://doi.org/10.1001/archneurol.2007.27>
- Fotos, A. F., Snyder, A. Z., Girton, L. E., Morris, J. C., & Buckner, R. L. (2005). Normative estimates of cross-sectional and longitudinal brain volume decline in aging and AD. *Neurology*, 64(6), 1032–1039. <https://doi.org/10.1212/01.WNL.0000154530.72969.11>
- Fushimi, Y., Miki, Y., Urayama, S. I., Okada, T., Mori, N., Hanakawa, T., ... & Togashi, K. (2007). Gray matter-white matter contrast on spin-echo T1-weighted images at 3 T and 1.5 T: a quantitative comparison study. *European radiology*, 17(11), 2921–2925. <https://doi.org/10.1007/s00330-007-0688-9>
- Ganzetti, M., Wenderoth, N., & Mantini, D. (2015). Mapping pathological changes in brain structure by combining T1-and T2-weighted MR imaging data. *Neuroradiology*, 57(9), 917–928. <https://doi.org/10.1007/s00234-015-1550-4>
- Gareau, P. J., Rutt, B. K., Karlik, S. J., & Mitchell, J. R. (2000). Magnetization transfer and multicomponent T2 relaxation measurements with histopathologic correlation in an experimental model of MS. *Journal of Magnetic Resonance Imaging: An Official Journal of the International Society for Magnetic Resonance in Medicine*, 11(6), 586–595. [https://doi.org/10.1002/1522-2586\(200006\)11:6<586::AID-JMRI3>3.0.CO;2-V](https://doi.org/10.1002/1522-2586(200006)11:6<586::AID-JMRI3>3.0.CO;2-V)
- Garza-Villarreal, E. A., Chakravarty, M. M., Hansen, B., Eskildsen, S. F., Devenyi, G. A., Castillo-Padilla, D., ... Patel, R. (2017). The effect of crack cocaine addiction and age on the microstructure and morphology of the human striatum and thalamus using shape analysis and fast diffusion kurtosis imaging. *Translational Psychiatry*, 7(5), e1122.
- Ge, Y., Grossman, R. I., Babb, J. S., Rabin, M. L., Mannon, L. J., & Kolson, D. L. (2002). Age-related total gray matter and white matter changes in normal adult brain. Part II: quantitative magnetization transfer ratio histogram analysis. *American Journal of Neuroradiology*, 23(8), 1334–1341.
- Giedd, J. N., Snell, J. W., Lange, N., Rajapakse, J. C., Casey, B. J., Kozuch, P. L., ... Rapoport, J. L. (1996). Quantitative magnetic resonance imaging of human brain development: Ages 4–18. *Cerebral Cortex*, 6(4), 551–559. <https://doi.org/10.1093/cercor/6.4.551>
- Glasser, M. F., Coalson, T. S., Robinson, E. C., Hacker, C. D., Harwell, J., Yacoub, E., ... Smith, S. M. (2016). A multi-modal parcellation of human cerebral cortex. *Nature*, 536(7615), 171–178.
- Glasser, M. F., Goyal, M. S., Preuss, T. M., Raichle, M. E., & Van Essen, D. C. (2014). Trends and properties of human cerebral cortex: Correlations with cortical myelin content. *NeuroImage*, 93, 165–175. <https://doi.org/10.1016/j.neuroimage.2013.03.060>

- Glasser, M. F., & Van Essen, D. C. (2011). Mapping human cortical areas in vivo based on myelin content as revealed by T1-and T2-weighted MRI. *Journal of Neuroscience*, 31(32), 11597–11616. <https://doi.org/10.1523/JNEUROSCI.2180-11.2011>
- Good, C. D., Johnsrude, I., Ashburner, J., Henson, R. N., Friston, K. J., & Frackowiak, R. S. (2001). Cerebral asymmetry and the effects of sex and handedness on brain structure: A voxel-based morphometric analysis of 465 normal adult human brains. *NeuroImage*, 14(3), 685–700. <https://doi.org/10.1006/nimg.2001.0857>
- Goodro, M., Sameti, M., Patenaude, B., & Fein, G. (2012). Age effect on subcortical structures in healthy adults. *Psychiatry Research: Neuroimaging*, 203(1), 38–45. <https://doi.org/10.1016/j.psychres.2011.09.014>
- Graybiel, A. M. (1995). Building action repertoires: Memory and learning functions of the basal ganglia. *Current Opinion in Neurobiology*, 5(6), 733–741.
- Graybiel, A. M. (2000). The basal ganglia. *Current Biology: CB*, 10(14), R509–R511.
- Greenberg, D. L., Messer, D. F., Payne, M. E., MacFall, J. R., Provenzale, J. M., Steffens, D. C., & Krishnan, R. R. (2008). Aging, gender, and the elderly adult brain: An examination of analytical strategies. *Neurobiology of Aging*, 29(2), 290–302. <https://doi.org/10.1016/j.neurobiolaging.2006.09.016>
- Grydeland, H., Walhovd, K. B., Tamnes, C. K., Westlye, L. T., & Fjell, A. M. (2013). Intracortical myelin links with performance variability across the human lifespan: Results from T1-and T2-weighted MRI myelin mapping and diffusion tensor imaging. *Journal of Neuroscience*, 33(47), 18618–18630. <https://doi.org/10.1523/JNEUROSCI.2811-13.2013>
- Guadalupe, T., Mathias, S. R., Theo, G. M., Whelan, C. D., Zwierns, M. P., Abe, Y., ... Aribisala, B. S. (2017). Human subcortical brain asymmetries in 15,847 people worldwide reveal effects of age and sex. *Brain Imaging and Behavior*, 11(5), 1497–1514. <https://doi.org/10.1007/s11682-016-9629-z>
- Gunning-Dixon, F. M., Head, D., McQuain, J., Acker, J. D., & Raz, N. (1998). Differential aging of the human striatum: A prospective MR imaging study. *American Journal of Neuroradiology*, 19(8), 1501–1507.
- Haacke, E. M., Cheng, N. Y., House, M. J., Liu, Q., Neelavalli, J., Ogg, R. J., ... Obenaus, A. (2005). Imaging iron stores in the brain using magnetic resonance imaging. *Magnetic Resonance Imaging*, 23(1), 1–25.
- Hagemeyer, J., Dwyer, M. G., Bergsland, N., Schweser, F., Magnano, C. R., Heininen-Brown, M., ... Polak, P. (2013). Effect of age on MRI phase behavior in the subcortical deep gray matter of healthy individuals. *AJNR. American Journal of Neuroradiology*, 34(11), 2144–2151. <https://doi.org/10.3174/ajnr.A3569>
- Hallgren, B., & Sourander, P. (1958). The effect of age on the non-haemin iron in the human brain. *Journal of Neurochemistry*, 3(1), 41–51.
- Halliday, G. M. (2009). Thalamic changes in Parkinson's disease. *Parkinsonism & Related Disorders*, 15, S152–S155. [https://doi.org/10.1016/S1353-8020\(09\)70804-1](https://doi.org/10.1016/S1353-8020(09)70804-1)
- Hannestad, J., Taylor, W. D., McQuoid, D. R., Payne, M. E., Krishnan, K. R. R., Steffens, D. C., & MacFall, J. R. (2006). White matter lesion volumes and caudate volumes in late-life depression. *International Journal of Geriatric Psychiatry*, 21(12), 1193–1198.
- Hasan, K. M., Halphen, C., Boska, M. D., & Narayana, P. A. (2008). Diffusion tensor metrics, T2 relaxation, and volumetry of the naturally aging human caudate nuclei in healthy young and middle-aged adults: Possible implications for the neurobiology of human brain aging and disease. *Magnetic Resonance in Medicine*, 59(1), 7–13. <https://doi.org/10.1002/mrm.21434>
- Howes, O. D., & Kapur, S. (2009). The dopamine hypothesis of schizophrenia: Version III—The final common pathway. *Schizophrenia Bulletin*, 35(3), 549–562. <https://doi.org/10.1093/schbul/sbp006>
- Inano, S., Takao, H., Hayashi, N., Yoshioka, N., Mori, H., Kunimatsu, A., ... Ohtomo, K. (2013). Effects of age and gender on neuroanatomical volumes. *Journal of Magnetic Resonance Imaging*, 37(5), 1072–1076. <https://doi.org/10.1002/jmri.23910>
- Inglese, M., & Ge, Y. (2004). Quantitative MRI: hidden age-related changes in brain tissue. *Topics in Magnetic Resonance Imaging*, 15(6), 355–363. <https://doi.org/10.1097/01.rmr.0000168069.12985.15>
- Ishida, T., Donishi, T., Iwatani, J., Yamada, S., Takahashi, S., Ukai, S., ... Kaneoke, Y. (2017). Elucidating the aberrant brain regions in bipolar disorder using T1-weighted/T2-weighted magnetic resonance ratio images. *Psychiatry Research: Neuroimaging*, 263, 76–84. <https://doi.org/10.1016/j.psychres.2017.03.006>
- Iwatani, J., Ishida, T., Donishi, T., Ukai, S., Shinosaki, K., Terada, M., & Kaneoke, Y. (2015). Use of T1-weighted/T2-weighted magnetic resonance ratio images to elucidate changes in the schizophrenic brain. *Brain and Behavior: A Cognitive Neuroscience Perspective*, 5(10), e00399. <https://doi.org/10.1002/brb3.399>
- Jack, C. R., Jr., Bernstein, M. A., Fox, N. C., Thompson, P., Alexander, G., Harvey, D., ... Dale, A. M. (2008). The Alzheimer's disease neuroimaging initiative (ADNI): MRI methods. *Journal of Magnetic Resonance Imaging*, 27(4), 685–691.
- Jahanshahi, M., Obeso, I., Rothwell, J. C., & Obeso, J. A. (2015). A fronto-striato-subthalamic-pallidal network for goal-directed and habitual inhibition. *Nature Reviews Neuroscience*, 16(12), 719. <https://doi.org/10.1038/nrn4038>
- Jäncke, L., Méritat, S., Liem, F., & Hänggi, J. (2015). Brain size, sex, and the aging brain. *Human Brain Mapping*, 36(1), 150–169. <https://doi.org/10.1002/hbm.22619>
- Janssen, R. J., Jylänki, P., Kessels, R. P., & van Gerven, M. A. (2015). Probabilistic model-based functional parcellation reveals a robust, fine-grained subdivision of the striatum. *NeuroImage*, 119, 398–405. <https://doi.org/10.1016/j.neuroimage.2015.06.084>
- Jernigan, T. L., Archibald, S. L., Fennema-Notestine, C., Gamst, A. C., Stout, J. C., Bonner, J., & Hesselink, J. R. (2001). Effects of age on tissues and regions of the cerebrum and cerebellum. *Neurobiology of Aging*, 22(4), 581–594. [https://doi.org/10.1016/S0197-4580\(01\)00217-2](https://doi.org/10.1016/S0197-4580(01)00217-2)
- Jones, D. K., Knösche, T. R., & Turner, R. (2013). White matter integrity, fiber count, and other fallacies: the do's and don'ts of diffusion MRI. *NeuroImage*, 73, 239–254. <https://doi.org/10.1016/j.neuroimage.2012.06.081>
- Keshavan, A., Datta, E., McDonough, I. M., Madan, C. R., Jordan, K., & Henry, R. G. (2018). Mindcontrol: A web application for brain segmentation quality control. *NeuroImage*, 170, 365–372. <https://doi.org/10.1016/j.neuroimage.2017.03.055>
- Knijnenburg, T. A., Wessels, L. F., Reinders, M. J., & Shmulevich, I. (2009). Fewer permutations, more accurate P-values. *Bioinformatics*, 25(12), i161–i168. <https://doi.org/10.1093/bioinformatics/btp211>
- Koo, M. S., Levitt, J. J., McCarley, R. W., Seidman, L. J., Dickey, C. C., Niznikiewicz, M. A., ... Shenton, M. E. (2006). Reduction of caudate nucleus volumes in neuroleptic-naïve female subjects with schizotypal personality disorder. *Biological Psychiatry*, 60(1), 40–48.
- Laule, C., Kozlowski, P., Leung, E., Li, D. K., MacKay, A. L., & Moore, G. W. (2008). Myelin water imaging of multiple sclerosis at 7 T: Correlations with histopathology. *NeuroImage*, 40(4), 1575–1580. <https://doi.org/10.1016/j.neuroimage.2007.12.008>
- Laule, C., Leung, E., Li, D. K., Traboulsee, A. L., Paty, D. W., MacKay, A. L., & Moore, G. W. (2006). Myelin water imaging in multiple sclerosis: Quantitative correlations with histopathology. *Multiple Sclerosis Journal*, 12(6), 747–753. <https://doi.org/10.1177/1352458506070928>
- Laule, C., Vavasour, I. M., Kolind, S. H., Li, D. K., Traboulsee, T. L., Moore, G. W., & MacKay, A. L. (2007). Magnetic resonance imaging of myelin. *Neurotherapeutics*, 4(3), 460–484. <https://doi.org/10.1016/j.nurt.2007.05.004>
- Lebel, C., Gee, M., Camicioli, R., Wieler, M., Martin, W., & Beaulieu, C. (2012). Diffusion tensor imaging of white matter tract evolution over

- the lifespan. *NeuroImage*, 60(1), 340–352. <https://doi.org/10.1016/j.neuroimage.2011.11.094>
- Lebel, C., Walker, L., Leemans, A., Phillips, L., & Beaulieu, C. (2008). Microstructural maturation of the human brain from childhood to adulthood. *NeuroImage*, 40(3), 1044–1055. <https://doi.org/10.1016/j.neuroimage.2007.12.053>
- Lee, K., Cherel, M., Budin, F., Gilmore, J., Consing, K. Z., Rasmussen, J., ... Buss, C. (2015, March). Early postnatal myelin content estimate of white matter via T1w/T2w ratio. In B. Gimi & A. Krol (Eds.), *Medical Imaging 2015: Biomedical applications in molecular, structural, and functional imaging, February 24–26, 2015, Orlando, FL* (Vol. 9417, p. 94171R). Bellingham, WA: International Society for Optics and Photonics. <https://doi.org/10.1117/12.2082198>
- Leh, S. E., Ptito, A., Chakravarty, M. M., & Strafella, A. P. (2007). Frontostriatal connections in the human brain: A probabilistic diffusion tractography study. *Neuroscience Letters*, 419(2), 113–118. <https://doi.org/10.1016/j.neulet.2007.04.049>
- Lemaître, H., Crivello, F., Grassiot, B., Alperovitch, A., Tzourio, C., & Mazoyer, B. (2005). Age- and sex-related effects on the neuroanatomy of healthy elderly. *NeuroImage*, 26(3), 900–911. <https://doi.org/10.1016/j.neuroimage.2005.02.042>
- Lerch, J. P., van der Kouwe, A. J., Raznahan, A., Paus, T., Johansen-Berg, H., Miller, K. L., ... Sotiropoulos, S. N. (2017). Studying neuroanatomy using MRI. *Nature Neuroscience*, 20(3), 314. <https://doi.org/10.1038/nn.4501>
- Levitt, J. J., McCarley, R. W., Dickey, C. C., Voglmaier, M. M., Niznikiewicz, M. A., Seidman, L. J., ... Shenton, M. E. (2002). MRI study of caudate nucleus volume and its cognitive correlates in neuroleptic-naïve patients with schizotypal personality disorder. *American Journal of Psychiatry*, 159(7), 1190–1197. <https://doi.org/10.1176/appi.ajp.159.7.1190>
- Mackay, A., Whittall, K., Adler, J., Li, D., Paty, D., & Graeb, D. (1994). In vivo visualization of myelin water in brain by magnetic resonance. *Magnetic resonance in medicine*, 31(6), 673–677. <https://doi.org/10.1002/mrm.1910310614>
- Madden, D. J., Bennett, I. J., Burzynska, A., Potter, G. G., Chen, N. K., & Song, A. W. (2012). Diffusion tensor imaging of cerebral white matter integrity in cognitive aging. *Biochimica et Biophysica Acta (BBA)-Molecular Basis of Disease*, 1822(3), 386–400. <https://doi.org/10.1016/j.bbadis.2011.08.003>
- Mädler, B., Drabycz, S. A., Kolind, S. H., Whittall, K. P., & MacKay, A. L. (2008). Is diffusion anisotropy an accurate monitor of myelination?: Correlation of multicomponent T2 relaxation and diffusion tensor anisotropy in human brain. *Magnetic resonance imaging*, 26(7), 874–888. <https://doi.org/10.1016/j.mri.2008.01.047>
- Makowski, C., Béland, S., Kostopoulos, P., Bhagwat, N., Devenyi, G. A., Malla, A. K., ... Chakravarty, M. M. (2018). Evaluating accuracy of striatal, pallidal, and thalamic segmentation methods: Comparing automated approaches to manual delineation. *NeuroImage*, 170, 182–198. <https://doi.org/10.1016/j.neuroimage.2017.02.069>
- Marnier, L., Nyengaard, J. R., Tang, Y., & Pakkenberg, B. (2003). Marked loss of myelinated nerve fibers in the human brain with age. *Journal of Comparative Neurology*, 462(2), 144–152.
- Middleton, F. A., & Strick, P. L. (2000). Basal ganglia output and cognition: Evidence from anatomical, behavioral, and clinical studies. *Brain and Cognition*, 42(2), 183–200. <https://doi.org/10.1006/brcg.1999.1099>
- Mungas, D., Gavett, B., Fletcher, E., Farias, S. T., DeCarli, C., & Reed, B. (2018). Education amplifies brain atrophy effect on cognitive decline: Implications for cognitive reserve. *Neurobiology of Aging*, 68, 142–150. <https://doi.org/10.1016/j.neurobiolaging.2018.04.002>
- Murphy, D. G., DeCarli, C., McIntosh, A. R., Daly, E., Mentis, M. J., Pietrini, P., ... Rapoport, S. I. (1996). Sex differences in human brain morphometry and metabolism: An in vivo quantitative magnetic resonance imaging and positron emission tomography study on the effect of aging. *Archives of General Psychiatry*, 53(7), 585–594.
- Narvacan, K., Treit, S., Camicioli, R., Martin, W., & Beaulieu, C. (2017). Evolution of deep gray matter volume across the human lifespan. *Human Brain Mapping*, 38(8), 3771–3790. <https://doi.org/10.1002/hbm.23604>
- Nauczyciel, C., Robic, S., Dondaine, T., Verin, M., Robert, G., Drapier, D., ... Millet, B. (2013). The nucleus accumbens: A target for deep brain stimulation in resistant major depressive disorder. *Journal of Molecular Psychiatry*, 1(1), 17. <https://doi.org/10.1186/2049-9256-1-17>
- Obeso, J. A., Rodriguez-Oroz, M. C., Rodriguez, M., Lanciego, J. L., Artieda, J., Gonzalo, N., & Olanow, C. W. (2000). Pathophysiology of the basal ganglia in Parkinson's disease. *Trends in Neurosciences*, 23, S8–S19.
- Odrobina, E. E., Lam, T. Y., Pun, T., Midha, R., & Stanisz, G. J. (2005). MR properties of excised neural tissue following experimentally induced demyelination. *NMR in Biomedicine*, 18(5), 277–284. <https://doi.org/10.1002/nbm.951>
- Østby, Y., Tamnes, C. K., Fjell, A. M., Westlye, L. T., Due-Tønnessen, P., & Walhovd, K. B. (2009). Heterogeneity in subcortical brain development: A structural magnetic resonance imaging study of brain maturation from 8 to 30 years. *Journal of Neuroscience*, 29(38), 11772–11782. <https://doi.org/10.1523/JNEUROSCI.1242-09.2009>
- Pardoe, H. R., Hiess, R. K., & Kuzniecky, R. (2016). Motion and morphometry in clinical and nonclinical populations. *NeuroImage*, 135, 177–185.
- Parent, A. (1990). Extrinsic connections of the basal ganglia. *Trends in Neurosciences*, 13(7), 254–258.
- Parent, A., & Hazrati, L. N. (1995). Functional anatomy of the basal ganglia. I. the Cortico-basal ganglia-Thalamo-cortical loop. *Brain Research. Brain Research Reviews*, 20(1), 91–127.
- Patenaude, B., Smith, S. M., Kennedy, D. N., & Jenkinson, M. (2011). A Bayesian model of shape and appearance for subcortical brain segmentation. *NeuroImage*, 56(3), 907–922. <https://doi.org/10.1016/j.neuroimage.2011.02.046>
- Pauli, W. M., O'Reilly, R. C., Yarkoni, T., & Wager, T. D. (2016). Regional specialization within the human striatum for diverse psychological functions. *Proceedings of the National Academy of Sciences of the United States of America*, 113(7), 1907–1912. <https://doi.org/10.1073/pnas.1507610113>
- Péran, P., Hagberg, G., Luccichenti, G., Cherubini, A., Brainovich, V., Celsis, P., ... Sabatini, U. (2007). Voxel-based analysis of R2* maps in the healthy human brain. *Journal of Magnetic Resonance Imaging*, 26(6), 1413–1420.
- Peters, A. (2002). The effects of Normal aging on myelin and nerve fibers: A review. *Journal of Neurocytology*, 31(8-9), 581–593.
- Pfefferbaum, A., Rohlfing, T., Rosenbloom, M. J., Chu, W., Colrain, I. M., & Sullivan, E. V. (2013). Variation in longitudinal trajectories of regional brain volumes of healthy men and women (ages 10 to 85 years) measured with atlas-based parcellation of MRI. *NeuroImage*, 65, 176–193. <https://doi.org/10.1016/j.neuroimage.2012.10.008>
- Pfefferbaum, A., Rohlfing, T., Rosenbloom, M. J., & Sullivan, E. V. (2012). Combining atlas-based parcellation of regional brain data acquired across scanners at 1.5 T and 3.0 T field strengths. *NeuroImage*, 60(2), 940–951. <https://doi.org/10.1016/j.neuroimage.2012.01.092>
- Pipitone, J., Park, M. T. M., Winterburn, J., Lett, T. A., Lerch, J. P., Pruessner, J. C., ... Alzheimer's Disease Neuroimaging Initiative. (2014). Multi-atlas segmentation of the whole hippocampus and subfields using multiple automatically generated templates. *NeuroImage*, 101, 494–512. <https://doi.org/10.1016/j.neuroimage.2014.04.054>
- Potvin, O., Mouih, A., Dieumegarde, L., Duchesne, S., & Alzheimer's Disease Neuroimaging Initiative. (2016). Normative data for subcortical regional volumes over the lifetime of the adult human brain. *NeuroImage*, 137, 9–20. <https://doi.org/10.1016/j.neuroimage.2016.05.016>
- Querbes, O., Aubry, F., Pariente, J., Lotterie, J. A., Démonet, J. F., Duret, V., ... Alzheimer's Disease Neuroimaging Initiative. (2009). Early diagnosis of Alzheimer's disease using cortical thickness: Impact of

- cognitive reserve. *Brain*, 132(8), 2036–2047. <https://doi.org/10.1093/brain/awp105>
- Randolph, C., Tierney, M. C., Mohr, E., & Chase, T. N. (1998). The repeatable battery for the assessment of neuropsychological status (RBANS): Preliminary clinical validity. *Journal of Clinical and Experimental Neuropsychology*, 20(3), 310–319. <https://doi.org/10.1076/jcen.20.3.310.823>
- Raz, N., Lindenberger, U., Rodrigue, K. M., Kennedy, K. M., Head, D., Williamson, A., ... Acker, J. D. (2005). Regional brain changes in aging healthy adults: General trends, individual differences and modifiers. *Cerebral Cortex*, 15(11), 1676–1689. <https://doi.org/10.1093/cercor/bhi044>
- Raz, N., & Rodrigue, K. M. (2006). Differential aging of the brain: Patterns, cognitive correlates and modifiers. *Neuroscience & Biobehavioral Reviews*, 30(6), 730–748. <https://doi.org/10.1016/j.neubiorev.2006.07.001>
- Raz, N., Rodrigue, K. M., Kennedy, K. M., Head, D., Gunning-Dixon, F., & Acker, J. D. (2003). Differential aging of the human striatum: Longitudinal evidence. *American Journal of Neuroradiology*, 24(9), 1849–1856.
- Raznahan, A., Shaw, P. W., Lerch, J. P., Clasen, L. S., Greenstein, D., Berman, R., ... Giedd, J. N. (2014). Longitudinal four-dimensional mapping of subcortical anatomy in human development. *Proceedings of the National Academy of Sciences of the United States of America*, 111(4), 1592–1597. <https://doi.org/10.1073/pnas.1316911111>
- Reuter, M., Tisdall, M. D., Qureshi, A., Buckner, R. L., van der Kouwe, A. J., & Fischl, B. (2015). Head motion during MRI acquisition reduces gray matter volume and thickness estimates. *NeuroImage*, 107, 107–115. <https://doi.org/10.1016/j.neuroimage.2014.12.006>
- Scheibe, S., & Carstensen, L. L. (2010). Emotional aging: Recent findings and future trends. *The Journals of Gerontology: Series B*, 65(2), 135–144. <https://doi.org/10.1093/geronb/gbp132>
- Seidler, R. D., Bernard, J. A., Burutolu, T. B., Fling, B. W., Gordon, M. T., Gwin, J. T., ... Lipps, D. B. (2010). Motor control and aging: Links to age-related brain structural, functional, and biochemical effects. *Neuroscience & Biobehavioral Reviews*, 34(5), 721–733. <https://doi.org/10.1016/j.neubiorev.2009.10.005>
- Shafee, R., Buckner, R. L., & Fischl, B. (2015). Gray matter myelination of 1555 human brains using partial volume corrected MRI images. *NeuroImage*, 105, 473–485. <https://doi.org/10.1016/j.neuroimage.2014.10.054>
- Shaw, P., De Rossi, P., Watson, B., Wharton, A., Greenstein, D., Raznahan, A., ... Chakravarty, M. M. (2014). Mapping the development of the basal ganglia in children with attention-deficit/hyperactivity disorder. *Journal of the American Academy of Child & Adolescent Psychiatry*, 53(7), 780–789. <https://doi.org/10.1016/j.jaac.2014.05.003>
- Shaw, P., Sharp, W., Sudre, G., Wharton, A., Greenstein, D., Raznahan, A., ... Rapoport, J. (2015). Subcortical and cortical morphological anomalies as an endophenotype in obsessive-compulsive disorder. *Molecular Psychiatry*, 20(2), 224. <https://doi.org/10.1038/mp.2014.3>
- Shehzad, Z., Giavasis, S., Li, Q., Benhajali, Y., Yan, C., Yang, Z., ... Craddock, C. (2015). The preprocessed connectomes project quality assessment protocol—A resource for measuring the quality of MRI data. *Frontiers in Neuroscience*. <https://doi.org/10.3389/conf.fnins.2015.91.00047>
- Solé-Padullés, C., Bartrés-Faz, D., Junqué, C., Vendrell, P., Rami, L., Clemente, I. C., ... Barrios, M. (2009). Brain structure and function related to cognitive reserve variables in normal aging, mild cognitive impairment and Alzheimer's disease. *Neurobiology of Aging*, 30(7), 1114–1124. <https://doi.org/10.1016/j.neurobiolaging.2007.10.008>
- Stanisz, G. J., Webb, S., Munro, C. A., Pun, T., & Midha, R. (2004). MR properties of excised neural tissue following experimentally induced inflammation. *Magnetic Resonance in Medicine: An Official Journal of the International Society for Magnetic Resonance in Medicine*, 51(3), 473–479. <https://doi.org/10.1002/mrm.20008>
- Stüber, C., Morawski, M., Schäfer, A., Labadie, C., Wähner, M., Leuze, C., ... Spemann, D. (2014). Myelin and iron concentration in the human brain: A quantitative study of MRI contrast. *NeuroImage*, 93, 95–106. <https://doi.org/10.1016/j.neuroimage.2014.02.026>
- Sullivan, E. V., Rosenbloom, M., Serventi, K. L., & Pfefferbaum, A. (2004). Effects of age and sex on volumes of the thalamus, pons, and cortex. *Neurobiology of Aging*, 25(2), 185–192. [https://doi.org/10.1016/S0197-4580\(03\)00044-7](https://doi.org/10.1016/S0197-4580(03)00044-7)
- Tamnes, C. K., Walhovd, K. B., Dale, A. M., Østby, Y., Grydeland, H., Richardson, G., ... Holland, D. (2013). Brain development and aging: Overlapping and unique patterns of change. *NeuroImage*, 68, 63–74. <https://doi.org/10.1016/j.neuroimage.2012.11.039>
- Tang, X., Holland, D., Dale, A. M., Younes, L., Miller, M. I., & Alzheimer's Disease Neuroimaging Initiative. (2014). Shape abnormalities of subcortical and ventricular structures in mild cognitive impairment and Alzheimer's disease: Detecting, quantifying, and predicting. *Human Brain Mapping*, 35(8), 3701–3725. <https://doi.org/10.1002/hbm.22431>
- Tang, Y., Nyengaard, J. R., Pakkenberg, B., & Gundersen, H. J. G. (1997). Age-induced white matter changes in the human brain: A stereological investigation. *Neurobiology of Aging*, 18(6), 609–615.
- Tardif, C. L., Gauthier, C. J., Steele, C. J., Bazin, P. L., Schäfer, A., Schaefer, A., ... Villringer, A. (2016). Advanced MRI techniques to improve our understanding of experience-induced neuroplasticity. *NeuroImage*, 131, 55–72. <https://doi.org/10.1016/j.neuroimage.2015.08.047>
- Tullo, S., Devenyi, G. A., Patel, R., Park, M. T. M., Collins, D. L., & Chakravarty, M. M. (2018). Warping an atlas derived from serial histology to 5 high-resolution MRIs. *Scientific Data*, 5, 180107. <https://doi.org/10.1038/sdata.2018.107>
- Tustison, N. J., Avants, B. B., Cook, P. A., Zheng, Y., Egan, A., Yushkevich, P. A., & Gee, J. C. (2010). N4ITK: Improved N3 bias correction. *IEEE Transactions on Medical Imaging*, 29(6), 1310–1320. <https://doi.org/10.1109/TMI.2010.2046908>
- Uddin, M. N., Figley, T. D., Marrie, R. A., Figley, C. R., & CCOMS Study Group. (2018). Can T1w/T2w ratio be used as a myelin-specific measure in subcortical structures? Comparisons between FSE-based T1w/T2w ratios, GRASE-based T1w/T2w ratios and multi-echo GRASE-based myelin water fractions. *NMR in Biomedicine*, 31(3), e3868. <https://doi.org/10.1002/nbm.3868>
- Uddin, M. N., Figley, T. D., Solar, K. G., Shatil, A. S., & Figley, C. R. (2019). Comparisons between multi-component myelin water fraction, T1w/T2w ratio, and diffusion tensor imaging measures in healthy human brain structures. *Scientific Reports*, 9(1), 2500. <https://doi.org/10.1038/s41598-019-39199-x>
- Van Der Werf, Y. D., Tisserand, D. J., Visser, P. J., Hofman, P. A., Vuurman, E., Uylings, H. B., & Jolles, J. (2001). Thalamic volume predicts performance on tests of cognitive speed and decreases in healthy aging: A magnetic resonance imaging-based volumetric analysis. *Cognitive Brain Research*, 11(3), 377–385.
- Volkow, N. D., Gur, R. C., Wang, G. J., Fowler, J. S., Moberg, P. J., Ding, Y. S., ... Logan, J. (1998). Association between decline in brain dopamine activity with age and cognitive and motor impairment in healthy individuals. *American Journal of Psychiatry*, 155(3), 344–349. <https://doi.org/10.1176/ajp.155.3.344>
- Wagenmakers, E. J., & Farrell, S. (2004). AIC model selection using Akaike weights. *Psychonomic Bulletin & Review*, 11(1), 192–196.
- Walhovd, K. B., Fjell, A. M., Reinvang, I., Lundervold, A., Dale, A. M., Eilertsen, D. E., ... Fischl, B. (2005). Effects of age on volumes of cortex, white matter and subcortical structures. *Neurobiology of Aging*, 26(9), 1261–1270. <https://doi.org/10.1016/j.neurobiolaging.2005.05.020>
- Walhovd, K. B., Westlye, L. T., Amlien, I., Espeseth, T., Reinvang, I., Raz, N., ... Dale, A. M. (2011). Consistent neuroanatomical age-related volume differences across multiple samples. *Neurobiology of*

- Aging, 32(5), 916–932. <https://doi.org/10.1016/j.neurobiolaging.2009.05.013>
- Wang, Q., Xu, X., & Zhang, M. (2010). Normal aging in the basal ganglia evaluated by eigenvalues of diffusion tensor imaging. *American journal of neuroradiology*, 31(3), 516–520. <https://doi.org/10.3174/ajnr.A1862>
- Watanabe, M., Liao, J. H., Jara, H., & Sakai, O. (2013). Multispectral quantitative MR imaging of the human brain: lifetime age-related effects. *Radiographics*, 33(5), 1305–1319. <https://doi.org/10.1148/rg.335125212>
- Webb, S., Munro, C. A., Midha, R., & Stanisz, G. J. (2003). Is multicomponent T2 a good measure of myelin content in peripheral nerve?. *Magnetic Resonance in Medicine: An Official Journal of the International Society for Magnetic Resonance in Medicine*, 49(4), 638–645. <https://doi.org/10.1002/mrm.10411>
- Weschler, D. (1999). *Weschler abbreviated scale of intelligence (WASI)*. London: Psychological Corporation.
- Wyciszkievicz, A., & Pawlak, M. A. (2014). Basal ganglia volumes: MR-derived reference ranges and lateralization indices for children and young adults. *The Neuroradiology Journal*, 27(5), 595–612. <https://doi.org/10.15274/NRJ-2014-10073>
- Xu, J., Kobayashi, S., Yamaguchi, S., Iijima, K. I., Okada, K., & Yamashita, K. (2000). Gender effects on age-related changes in brain structure. *American Journal of Neuroradiology*, 21(1), 112–118.
- Xu, X., Wang, Q., & Zhang, M. (2008). Age, gender, and hemispheric differences in iron deposition in the human brain: An in vivo MRI study. *NeuroImage*, 40(1), 35–42. <https://doi.org/10.1016/j.neuroimage.2007.11.017>
- Yeatman, J. D., Wandell, B. A., & Mezer, A. A. (2014). Lifespan maturation and degeneration of human brain white matter. *Nature communications*, 5, 4932. <https://doi.org/10.1038/ncomms5932>
- Yin, H. H., & Knowlton, B. J. (2006). The role of the basal ganglia in habit formation. *Nature Reviews Neuroscience*, 7(6), 464. <https://doi.org/10.1038/nrn1919>
- Yushkevich, P. A., Piven, J., Hazlett, H. C., Smith, R. G., Ho, S., Gee, J. C., & Gerig, G. (2006). User-guided 3D active contour segmentation of anatomical structures: Significantly improved efficiency and reliability. *NeuroImage*, 31(3), 1116–1128. <https://doi.org/10.1016/j.neuroimage.2006.01.015>
- Ziegler, G., Dahnke, R., Jäncke, L., Yotter, R. A., May, A., & Gaser, C. (2012). Brain structural trajectories over the adult lifespan. *Human Brain Mapping*, 33(10), 2377–2389. <https://doi.org/10.1002/hbm.21374>

SUPPORTING INFORMATION

Additional supporting information may be found online in the Supporting Information section at the end of this article.

How to cite this article: Tullo S, Patel R, Devenyi GA, et al. MR-based age-related effects on the striatum, globus pallidus, and thalamus in healthy individuals across the adult lifespan. *Hum Brain Mapp*. 2019;40:5269–5288. <https://doi.org/10.1002/hbm.24771>